USGS
science for a changing world

Fate and Transport Modeling of Selected Chlorinated Organic Compunds at Hangar 1000, U.S. Naval Air Station, Jacksonville, Florida

U.S. Geological Survey
Water Resources Investigations Report 03-4089

Prepared as part of the
U.S. Navy, Southern Division,
Naval Facilities Engineering Command

Fate and Transport Modeling of Selected Chlorinated Organic Compounds at Hangar 1000, U.S. Naval Air Station, Jacksonville, Florida

By J. Hal Davis

U.S. Geological Survey

Water-Resources Investigations Report 03-4089

Prepared in cooperation with the

U.S. NAVY, SOUTHERN DIVISION,

NAVAL FACILITIES ENGINEERING COMMAND

science for a changing world

Tallahassee, Florida
2003

U.S. DEPARTMENT OF THE INTERIOR
GALE A. NORTON, Secretary

U.S. GEOLOGICAL SURVEY
Charles G. Groat, Director

For additional information write to:

U.S. Geological Survey
2010 Levy Avenue
Tallahassee, FL 32310

Copies of this report can be purchased from:

U.S. Geological Survey
Branch of Information Services
Box 25286
Denver, CO 80225-0286
888-ASK-USGS

Additional information about water resources in Florida is available on the internet at **http://fl.water.usgs.gov**

CONTENTS

FIGURES

TABLES

CONVERSION FACTORS, DATUMS, AND ABBREVIATIONS

Multiply	By	To obtain
inch (in.)	25.4	millimeter (mm)
foot (ft)	0.3048	meter (m)
mile (mi)	1.609	kilometer (km)
inch per year (in/yr)	25.4	millimeter per year (mm/yr)
square foot (ft^2)	0.09290	square meter (m^2)
square mile (mi^2)	2.59	square kilometer (km^2)
foot per day (ft/d)	0.3048	meter per day (m/d)
foot squared per day (ft^2/d)	0.0929	meter squared per day (m^2/d)
cubic foot per day (ft^3/d)	0.028317	cubic meter per day (m^3/d)
cubic foot per second (ft^3/s)	0.02832	cubic meter per second (m^3/s)
foot per year (ft/yr)	0.3048	meter per year (m/yr)

ACRONYMS AND ABBREVIATIONS

DCE	Dichloroethene
g/cm3	grams per cubic centimeter
µg/L	micrograms per liter
MODFLOW	Modular Three-Dimensional Finite-Difference Ground-Water Flow Model
OU1	Operable Unit 1
RT3D	Reactive Transport in Three Dimensions
TCE	Trichloroethene
USEPA	U.S. Environmental Protection Agency
USGS	U.S. Geological Survey
VC	Vinyl Chloride

Vertical coordinate information is referenced to the National Geodetic Vertical Datum of 1929 (NGVD29); horizontal coordinate information is referenced to the North American Datum of 1927 (NAD27).

Fate and Transport Modeling of Selected Chlorinated Organic Compounds at Hangar 1000, U.S. Naval Air Station, Jacksonville, Florida

By J. Hal Davis

ABSTRACT

The Jacksonville Naval Air Station occupies 3,800 acres adjacent to the St. Johns River in Jacksonville, Florida. Two underground storage tanks at Hangar 1000 contained solvents from the late 1960s until they were removed in 1994. Ground-water samples at one of the tank sites had levels of trichloroethene (TCE) and total dichloroethene (DCE) of 8,710 micrograms per liter (μg/L) and 4,280 μg/L, respectively. Vinyl chloride (VC) at the site is the result of the biodegradation of DCE. Ground water beneath Hangar 1000 flows toward a storm sewer. TCE and DCE plumes travel with the ground water and presumably have reached the storm sewer, which discharges to the St. Johns River.

Simulation of solute transport indicates that the traveltime from the storage tank site to the storm sewer is 16, 14, and 12 years for TCE, DCE, and VC respectively. TCE has the longest traveltime because it has the highest retardation factor at 2.5, DCE takes less time with a retardation factor of 2.0, and VC has the quickest traveltime because it has the lowest retardation factor of 1.7. Based on modeling results, the release of contaminants in the aquifer occurred more than 16 years ago.

Model-derived dispersivity values at Hangar 1000 were: longitudinal 1.5 feet (ft), transverse 0.27 ft, and vertical 0.27 ft. The model-derived first order decay rates for biodegradation of TCE, DCE, and VC were 0.0002 per day (d^{-1}), 0.0002 d^{-1}, and 0.06 d^{-1}, respectively. These rates are equivalent to half-lives of 13.7 years for TCE and DCE and 17 days for VC.

Source area reductions in contaminant concentrations of 50 and 100 percent were modeled to simulate remediation. As expected, reducing the source concentration by 50 percent resulted in eventual TCE, DCE, and VC concentrations that were half of the original concentrations. About 16 years were needed for new steady-state TCE concentrations to develop, about 14 years for DCE, and about 12 years for VC. Reducing the source area concentrations by 100 percent in the model eventually resulted in zero concentrations of TCE, DCE, and VC. The modeled period of time for the contaminants to be removed from the aquifer once the source was removed was about 17 years for TCE, 15 years for DCE, and 13 years for VC.

INTRODUCTION

The U.S. Naval Air Station, (referred to as the Station) occupies 3,800 acres adjacent to the St. Johns River in Jacksonville, Fla. *(*fig. 1*).* The mission of the Station is to provide aerial anti-submarine warfare support, aviator training, and aircraft maintenance. Support facilities at the Station include an airfield, a maintenance depot, a Naval hospital, a Naval supply center, and recreational and residential facilities. Military activities have been conducted at the Station since 1909; the Station presently employs about 15,000 people.

The Station was placed on the U.S. Environmental Protection Agency's (USEPA) National Priorities List in December 1989, and is participating in the U.S. Department of Defense Installation Restoration Program, which serves to identify and remediate environmental contamination in compliance with the Comprehensive Environmental Response, Compensation, and Liability Act and the Superfund Amendments and Reauthorization Act of 1980 and 1985, respectively. On October 23, 1990, the Station entered into a Federal Facility Agreement with the USEPA and the Florida Department of Environmental Protection, which designated Operable Units 1, 2, and 3 at the Station (U.S. Navy, 1994a). Operable Units (fig. 1) were designated in areas where several sources of similar contamination existed in close proximity, thus allowing the contaminated areas to be addressed in one coordinated effort. Operable Unit 1 (OU1) was the Station landfill; this site has been discussed in previous studies (Davis and others, 1996). Operable Unit 2 (OU2) was the wastewater treatment plant, which has been remediated. Operable Unit 3 (OU3) was the Naval Aviation Depot; this site has been discussed in previous studies (Davis, 1998; 2000). Since entering into the Federal Facility Agreement, several additional operable units have been designated, including Operable Unit 6 (OU6), also known as Hangar 1000, which is the subject of this report.

Aircraft are serviced and repaired at Hangar 1000. To contain the solvents used at the hangar, two underground storage tanks were operated from the late 1960s until their use was discontinued in 1994. One tank was a 750-gallon concrete tank used as a solvent and water separator. The other was a 2,000-gallon steel tank, which received solvent overflow from the first tank as well as waste oils and solvents discharged from other operations at the facility. Both tanks, associated piping systems, and visually contaminated soils were excavated and removed in March 1994. After removal, contamination levels in the wells near the removal site fluctuated, indicating that tank removal may have spread the contamination (U.S. Navy, in press.) Floor drains and their associated pipes were abandoned intact at the time of the tank removals.

The Navy has documented the occurrence and distribution of contamination at Hangar 1000 through a contractor, Tetra Tech NUS, Inc. (Tetra Tech). Currently, Tetra Tech is determining whether the contamination poses a risk to human health or the environment. To better understand the fate and transport and consequences of future remedial actions on contamination at Hanger 1000, the U.S. Geological Survey (USGS) conducted a study to simulate the movement of contaminated ground water from the old storage tank site to ground-water discharge areas.

Purpose and Scope

A computer model capable of simulating the ground-water flow and the fate and transport of trichloroethene (TCE), dichloroethene (DCE), and vinyl chloride (VC) in the ground water at Hangar 1000 was needed by the Navy to aid in remedial decisions. The purpose of this report is to document the development of this model, which simulates ground-water flow and solute transport, and present the results of the model predictions. The computer modeling effort consisted of: (1) updating an existing large-scale ground-water model to simulate ground-water flow in the vicinity of Hangar 1000, (2) establishing boundary conditions for a site-specific model with the large-scale model, and (3) predicting the movement of contaminants at Hangar 1000 through solute transport simulation using the site-specific model.

Previous Modeling at the Jacksonville Naval Air Station

The USGS previously developed and calibrated a one-layer regional ground-water flow model that simulated steady-state flow in the surficial aquifer that underlies the site (Davis and others, 1996). This model used the USGS Modular Three-Dimensional Finite-Difference Ground-Water Flow Model (MODFLOW) software as described in McDonald and Harbaugh (1988). The regional model had 240 rows and 290 columns with a uniform cell size of 100 by

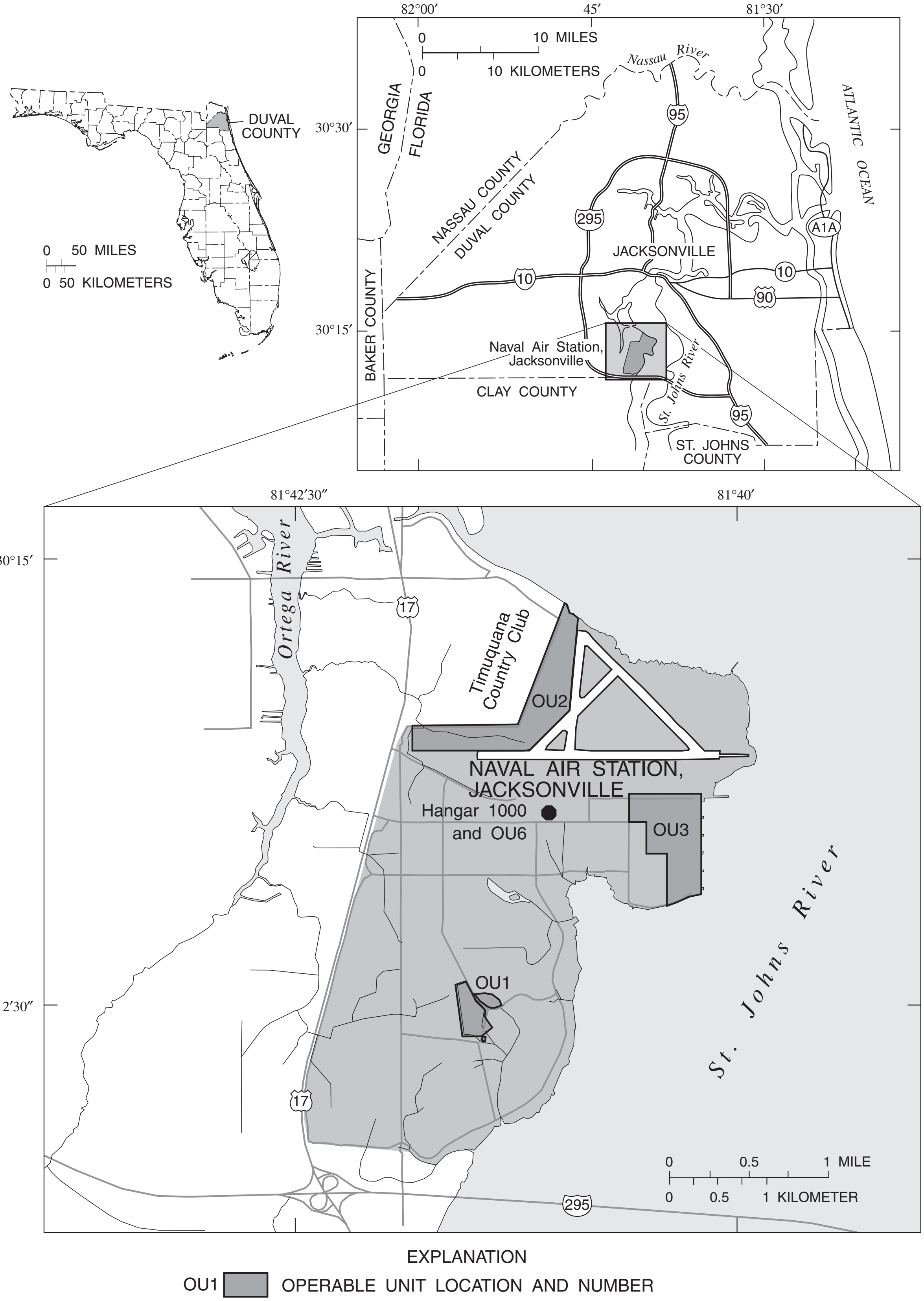

Figure 1. Location of the Jacksonville Naval Air Station.

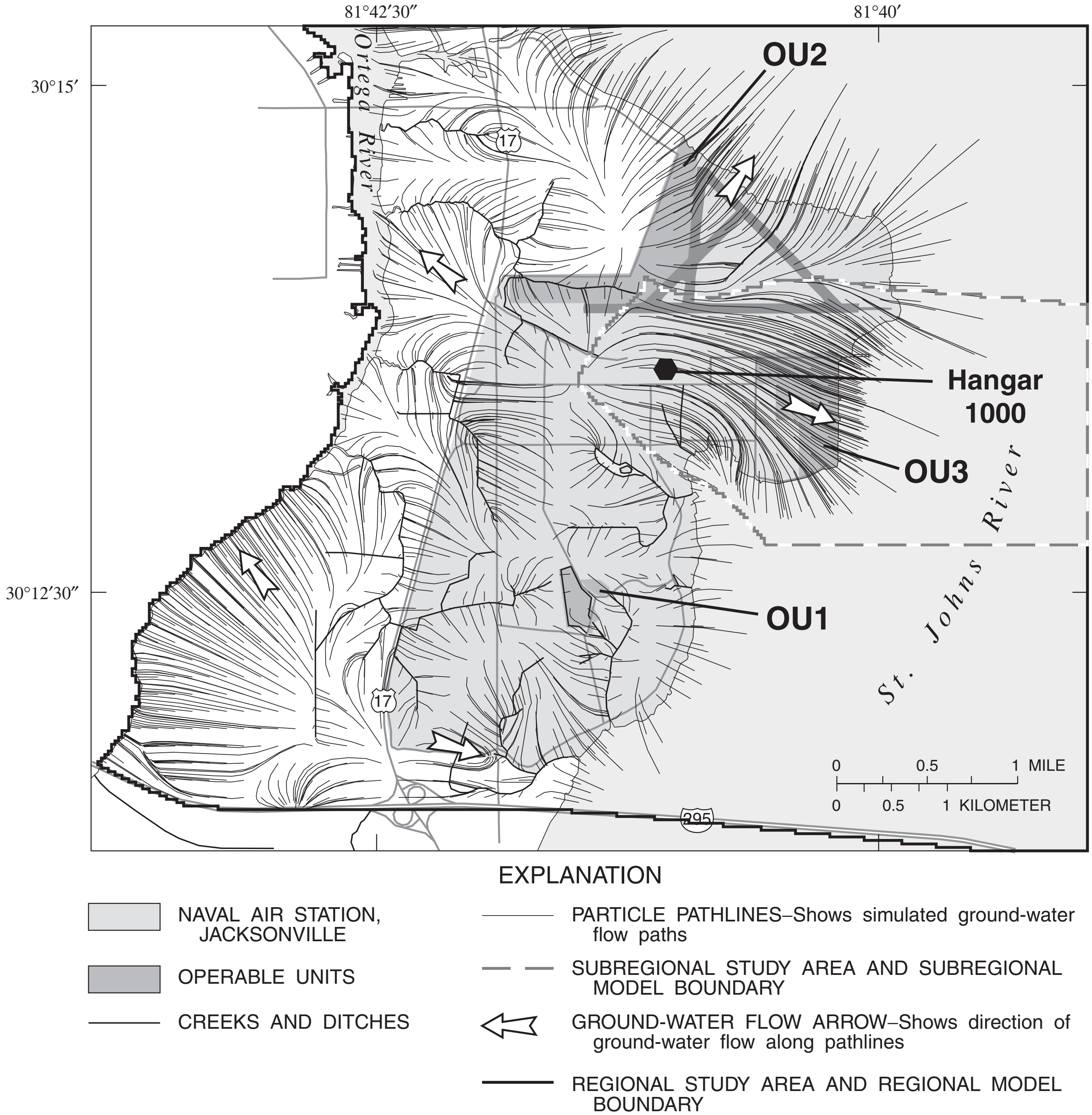

Figure 2. Subregional and regional model areas with particle pathlines.

100 feet (ft), and simulated steady-state flow at the entire Station and some surrounding areas (fig. 2). The model was used to determine the direction and velocity of ground-water flow throughout the Station as well as to evaluate the effect of proposed remediation scenarios on ground-water flow at OU1. Later, this model was used to establish boundary conditions for a smaller subregional model centered at OU3.

The subregional ground-water flow model (Davis, 1998) was developed to investigate steady-state ground-water flow at OU3. Boundaries for the regional and subregional model are shown in figure 2. The subregional model had 2 layers with 78 rows and 148 columns and a uniform cell size of 100 by 100 ft. This model was used to establish the boundary conditions and aquifer properties for a site-specific solute-transport model at OU3 (Davis, 2000), and to predict the movement of TCE, DCE, and VC from OU3 to the ultimate discharge points in the St. Johns River. The solute transport modeling was conducted using the Modular Three-Dimensional Multi-Species Transport Model (Zheng and Wang, 1998) computer software.

Acknowledgments

The author expresses appreciation to Dana Gaskins, Cliff Casey, and Anthony Robinson of U.S. Navy, Southern Division, Naval Facilities Engineering Command for providing information and funding; Tim Curtin and Jane Beason of the Station for helping provide access to Station facilities; and Greg Roof and Mark Peterson of Tetra Tech for providing technical assistance and data.

Methods

For this study, a ground-water flow model previously developed to simulate ground-water flow at OU3 was updated and used to simulate ground-water flow at Hangar 1000. This model was documented by Davis (2000). The updated model was then used to set the boundary conditions for a site-specific solute transport model. All of the models referenced were based on previous work conducted by the USGS. All of the water-quality sampling data was collected by Tetra Tech, and thus, the discussion of contamination distribution, history, and movement is based on Tetra Tech data. For a more complete discussion of the methods and results determined by Tetra Tech, see U.S. Navy (in press).

HYDROLOGIC SETTING

The climate for Jacksonville is humid subtropical, with an average annual rainfall and temperature for 1967-96 of 60.63 inches and 78 °F, respectively. Most of the annual rainfall occurs in late spring and early summer (Fairchild, 1972). Rainfall distribution is highly variable because most comes from scattered convective thunderstorms during the summer. Winters are mild and dry with occasional frost from November through February (Fairchild, 1972).

Land-surface topography consists of gently rolling hills with elevations ranging from about 30 ft above sea level on hilltops to 1 ft above sea level at the shorelines of the St. Johns and Ortega Rivers (fig. 1). The Naval Air Station is located in the Dinsmore Plain of the Northern Coastal Strip of the Sea Island District

<table>
<tr><th rowspan="2">SYSTEM</th><th rowspan="2">SERIES</th><th rowspan="2">FORMATION</th><th rowspan="2">HYDROGEOLOGIC UNIT</th><th colspan="3">MODEL LAYERS</th></tr>
<tr><th>REGIONAL MODEL</th><th>PREVIOUS SUBREGIONAL MODEL DOCUMENTED BY DAVIS (1998)</th><th>HANGER 1000 SUBREGIONAL MODEL, OU3 SUBREGIONAL MODEL, AND HANGER 1000 SITE-SPECIFIC SOLUTE TRANSPORT MODEL</th></tr>
<tr><td rowspan="3">QUATERNARY</td><td>HOLOCENE</td><td rowspan="4">Undifferentiated terrace and shallow marine deposits</td><td rowspan="4">Surficial aquifer</td><td rowspan="4">Layer 1</td><td rowspan="2">Layer 1 (Upper layer)
See Note "A"</td><td>Layer 1 (Upper layer)</td></tr>
<tr><td rowspan="2">PLEISTOCENE</td><td>Layer 2 (Clay layer)</td></tr>
<tr><td rowspan="2">Layer 2 (Intermediate layer)</td><td>Layer 3 (Intermediate layer)</td></tr>
<tr><td rowspan="2">TERTIARY</td><td>PLIOCENE</td><td>Layer 4 (Intermediate layer)</td></tr>
<tr><td>MIOCENE</td><td>Hawthorn Group</td><td>Confining unit</td><td>No-flow boundary</td><td>No-flow boundary</td><td>No-flow boundary</td></tr>
</table>

Note A: The clay between layers 1 and 2 was simulated by a low vertical conductance.

EXPLANATION

SURFICIAL AQUIFER

Figure 3. Geologic units, hydrologic units, and equivalent layers used in the computer model.

in the Atlantic Coastal Plain Section (Brooks, 1981). The Dinsmore Plain is characterized by low-relief, clastic terrace deposits of Pleistocene to Holocene age (Brooks, 1981).

The surficial aquifer is exposed at land surface and forms the uppermost permeable unit at the Station. The aquifer is composed of sedimentary deposits of Pliocene to Holocene age (fig. 3), and consists of 30 to 100 ft of tan to yellow, medium to fine unconsolidated silty sands interbedded with lenses of clay, silty clay, and sandy clay (U.S. Navy, 1994a). The Pleistocene-age sedimentary deposits in Florida were deposited in a series of terraces formed during marine transgressions and regressions associated with glacial and interglacial periods (Miller, 1986).

The surficial aquifer is composed of three distinct layers in the vicinity of Hangar 1000 and 0U3 (fig. 4). The upper layer is unconfined and extends from land surface to depths of about 15 to 35 ft below land surface (Navy, 1998). Beneath the upper layer (in most areas) is a low-permeability clay layer (figs. 4 and 5). This clay layer, where present, separates the upper layer of the surficial aquifer from the intermediate layer. In areas where this clay layer is 5 to 30 ft thick (fig. 5), it is almost exclusively clay; where the layer is greater than 30 ft thick, it grades into a silt and clay mixture at depth. The extent of the clay is well known at OU3 because of the extensive wells and direct push drilling that was conducted in association with contaminant delineation. The westward extent of the clay toward Hangar 1000 is less well known; however, a relatively thick clay (5 to 20 ft) is present at Hangar 1000. For this reason, it is speculated that the clay at Hangar 1000 and OU3 are connected. In any event, the relatively thick, dense clay at Hangar 1000 separates the surficial aquifer into two separate flow zones at the site.

The confined intermediate layer (fig. 4) extends below the clay downward to the top of the Hawthorn Group. The base of the surficial aquifer is formed by the top of the Miocene-age Hawthorn Group (figs. 4 and 6), which is mainly composed of low-permeability clays (Scott, 1988).

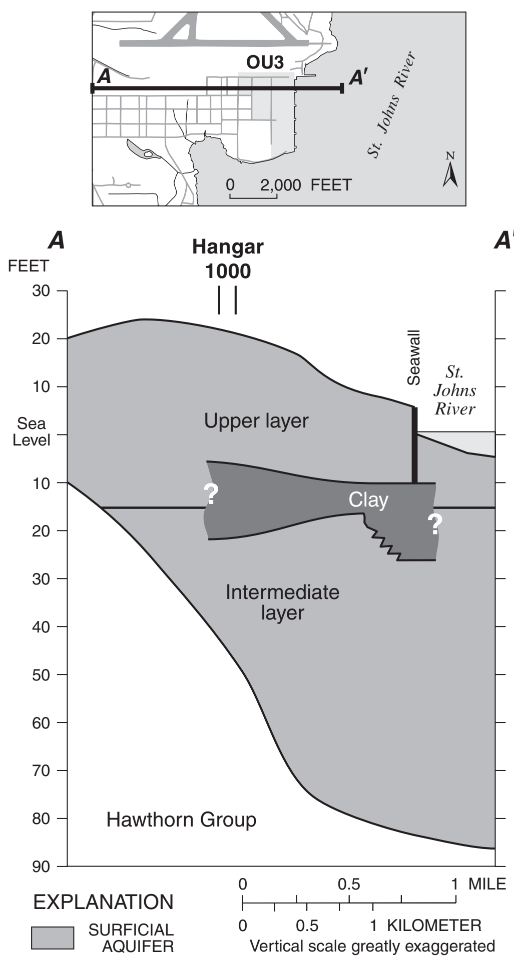

Figure 4. Generalized hydrogeologic section through the subregional study area.

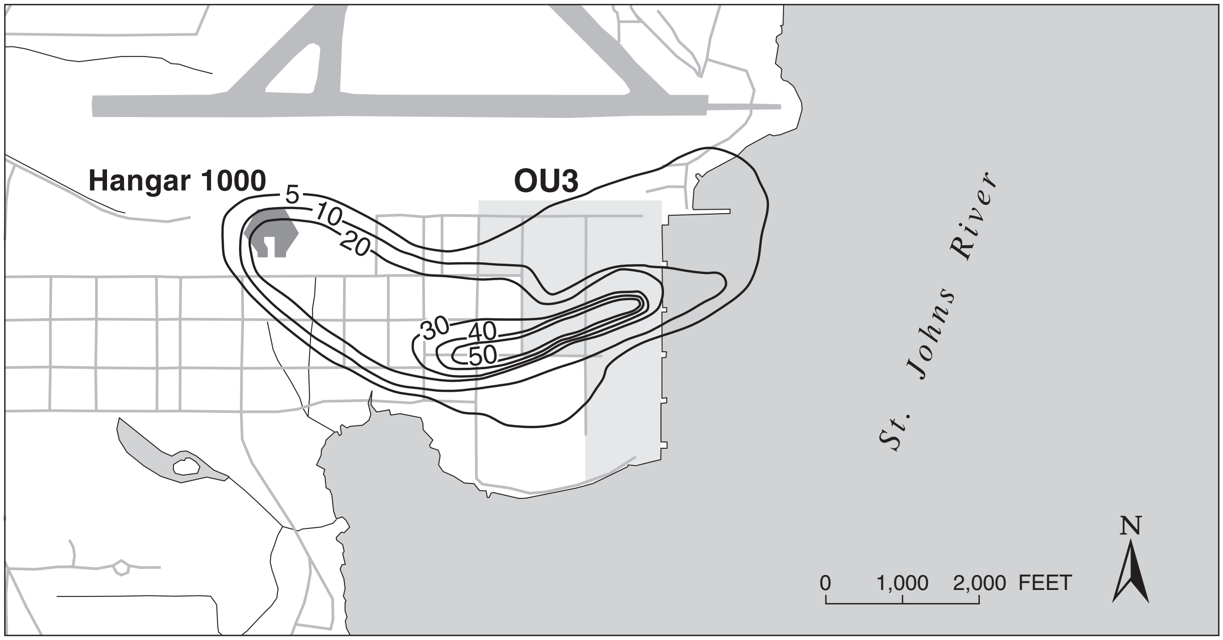

EXPLANATION

—5— LINE OF EQUAL THICKNESS OF CLAY LAYER–In feet above NGVD of 1929. Contour interval 5 and 10 feet

Figure 5. Extent and thickness of the clay layer that separates the upper and intermediate layers of the surficial aquifer.

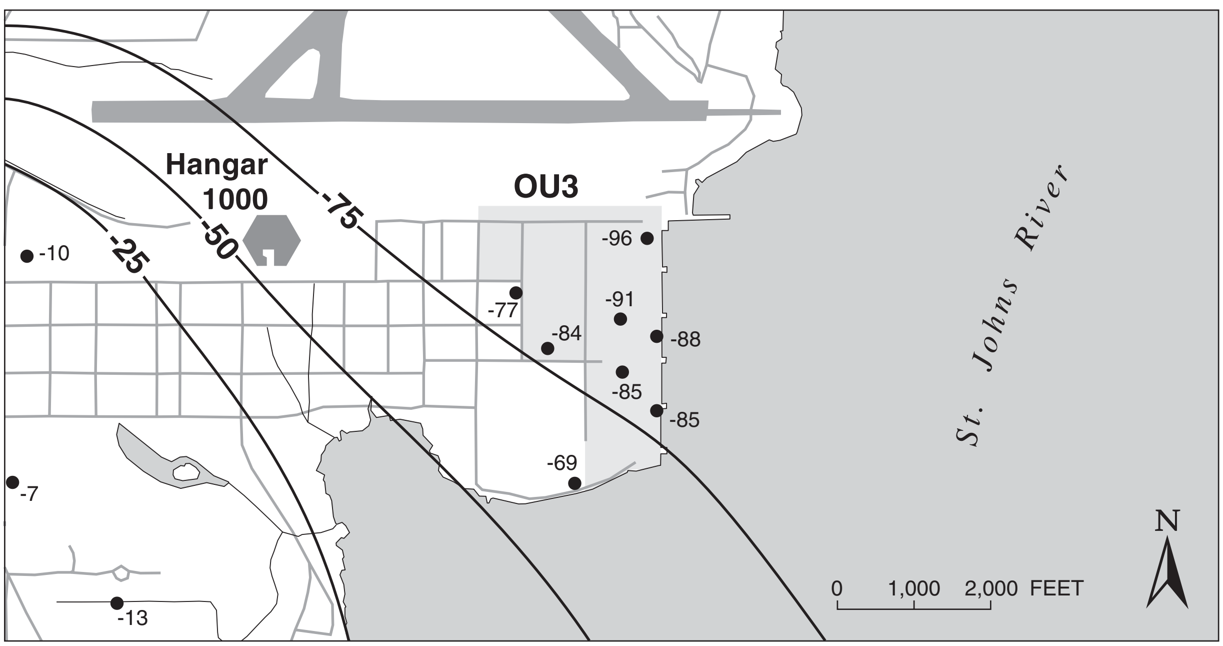

EXPLANATION

—-25— STRUCTURE CONTOUR–Shows altitude of the top of the Hawthorn Group. Contour interval is 25 feet. Datum is NGVD of 1929

● -13 WELL–Number is the altitude of the top of the Hawthorn Group in feet below NGVD of 1929

Figure 6. Top of the Hawthorn Group.

The top of the Hawthorn Group ranges from 35 to 100 ft below land surface at the Station and is about 60 ft below land surface at Hangar 1000. The Hawthorn Group is approximately 300 ft thick and composed of dark gray and olive-green sandy to silty clay, clayey sand, clay, and sandy limestone, all containing moderate to large amounts of black phosphatic sand, granules, or pebbles (Fairchild, 1972; Scott, 1988).

Wells used to define the water-table surface are shown in figure 7 and listed in table 1; wells used to define the potentiometric surface in the intermediate layer are shown in figure 8 and listed in table 2. The water-table surface on April 4, 2001, is shown in figure 9. In general, the water table slopes eastward toward the St. Johns River. However, this eastward slope is modified by the presence of leaky storm drains throughout the study area and two small ditches south of Hanger 1000.

An extensive stormwater-drainage system is present at the Station (fig. 10). The maintenance staff and consultants performed photographic surveys at OU3 documenting that ground-water seeps into the drains through joints and cracks in the drainage pipes (U.S. Navy, written commun., 1999.) Visual inspection of the drains by Navy personnel indicated that the leakage is generally confined to high motor-traffic areas. Drain depths vary, but generally range from 5 to 10 ft below land surface. All drains are in the upper layer of the aquifer.

The locations of sewer sections that drain ground water from the surficial aquifer are shown in figure 11, and the water-table surface in the vicinity of Hangar 1000 on April 4, 2001, is shown in figure 12. The water table in the vicinity of Hangar 1000 slopes southeastward toward storm drains. The ground-water contours wrap around sewer section 4 (fig. 12), indicating that ground water from the surficial aquifer is discharging to the storm drain from both sides. South of Hanger 1000, the water table slopes toward the small ditch southeast of Hangar 1000, indicating that water is discharging from the aquifer to the ditch from both sides. These ditches were concrete-lined in the 1940s by German prisoners of war; however, the linings presently contain numerous cracks and openings.

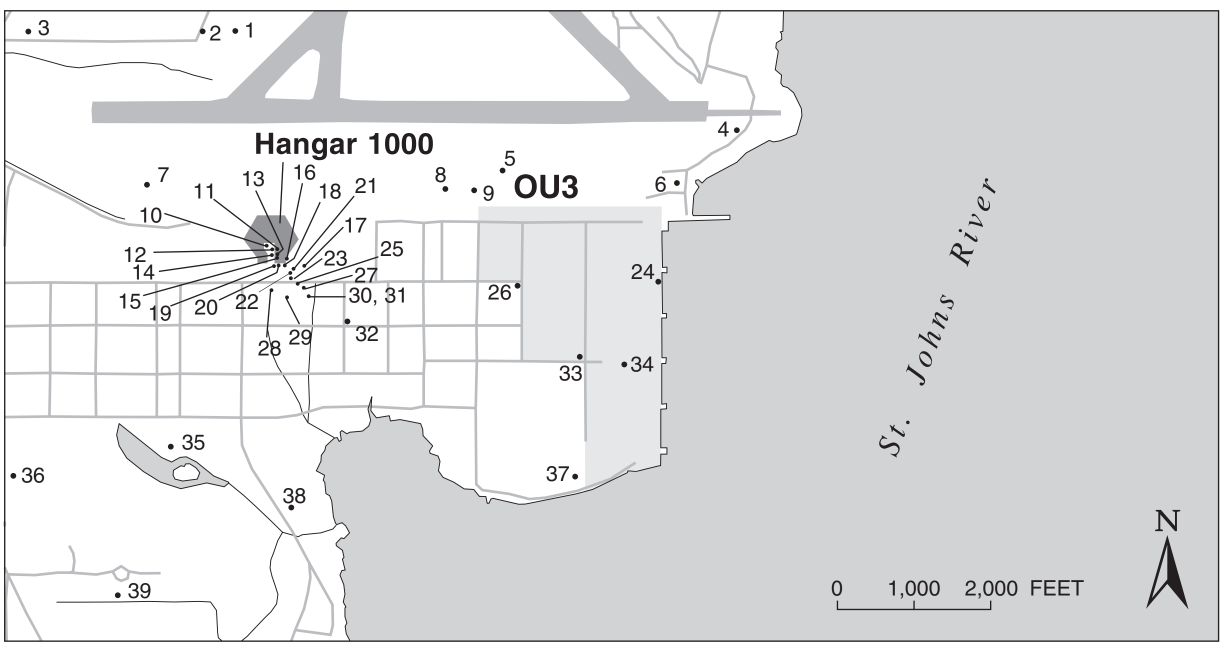

EXPLANATION

• 39 UPPER LAYER WELL WITH NUMBER–Number corresponds to map number in table 1

Figure 7. Wells completed in the upper layer of the surficial aquifer within the subregional study area.

Table 1. Monitoring wells completed in the upper layer of the surficial aquifer

Map number (see figure 7)	Well name	Altitude of top of casing, in feet	Well depth, in feet	Altitude of head on April 4, 2001, in feet
1	MW-16	20.68	12.00	15.50
2	PZ-1	19.15	14.00	15.16
3	PZ-6	19.13	15.90	10.57
4	JAX-TF-MW27	6.20	9.00	4.53
5	JAX-HA-MW03	10.04	12.00	6.79
6	JAX-TF-MW14	8.65	11.00	4.46
7	MW41-R	21.29	18.40	16.28
8	JAX-HA-MW05	11.11	12.00	7.96
9	JAX-HA-MW06	10.23	12.00	7.14
10	H10-MW10	16.37	14.00	9.72
11	H10-MW07	16.93	14.00	9.48
12	H10-MW08	16.46	14.00	9.54
13	H10-MW06	16.96	14.00	9.36
14	H10-MW02	16.19	14.00	9.47
15	H10-MW05	16.93	14.00	9.28
16	H10-MW15	15.67	15.00	9.00
17	H10-MW20	12.28	11.00	10.48
18	H10-MW14	16.35	15.00	8.93
19	H10-MW03	16.40	14.00	9.30
20	H10-MW13	16.56	15.00	9.17
21	H10-MW18	14.48	21.00	8.88
22	H10-MW22	14.17	11.70	8.27
23	H10-MW17	14.13	21.00	7.82
24	PZOO4	5.64	14.00	1.95
25	H10-MW19	14.24	12.00	6.74
26	PZO26	10.86	13.50	4.96
27	H10-MW23	12.62	15.00	5.73
28	H10-MW25	16.38	11.00	9.00
29	H10-MW24	17.01	14.50	8.38
30	H10-MW26	9.50	25.00	5.90
31	H10-MW27	9.70	14.00	6.47
32	MW-122	13.67	13.50	10.04
33	PZO17	10.77	14.00	3.76
34	PZO12	9.22	15.00	2.09
35	MW-47	20.99	14.50	14.42
36	MW-45	27.45	16.00	20.07
37	MW-49	22.11	25.50	1.81
38	MW-121	11.47	13.50	7.09
39	MW-52	27.76	16.00	18.18

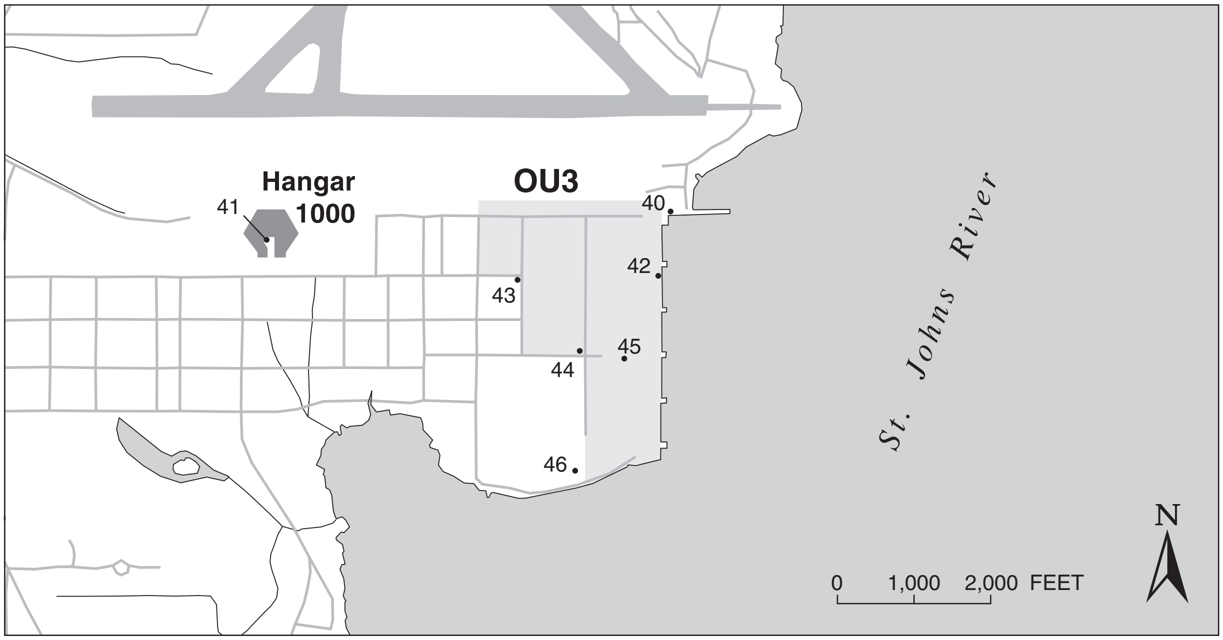

EXPLANATION

• 46 INTERMEDIATE LAYER WELL WITH NUMBER–Number corresponds to map number in table 2

Figure 8. Wells completed in the intermediate layer of the surficial aquifer within the subregional study area.

Table 2. Monitoring wells completed in the intermediate layer of the surficial aquifer

Map number (see figure 8)	Well name	Altitude of top of casing, in feet	Well depth, in feet	Altitude of head on April 4, 2001, in feet
40	JAX-TF-MW48D	8.36	36.50	2.23
41	H10-MW11	16.35	39.00	9.87
42	PZOO3	5.71	63.70	3.65
43	PZO25	10.69	85.50	5.85
44	PZO16	10.80	54.00	2.64
45	PZO11	9.27	93.00	2.01
46	MW-50	21.96	92.00	1.96

Storm sewer section 2 has several steel grates that allow observation of the sewer. In some parts of the sewer, sand boils can be seen at joints where ground water is leaking in. The drains were observed during dry periods; however, not all of the water flowing in the drains could be attributed to ground-water leakage, because parts of sewer section 2 are connected to overflow-underflow weirs that are connected to wash racks that drain to section 2. Other drains were difficult to observe except at a few occasional manholes. Sections 1 and 5 were almost completely unobservable; however, some observations of the sewer could be made at section 4 through the manholes. Observations through a manhole at the junction of sections 2, 4, and 5 indicated that water in the drain flowed southward but did not enter section 4 because a small berm blocked the flow. Further eastward, a small flow was observed through other manholes along section 4, presumably from ground-water inflow to the drain system. However, no direct evidence such as sand boils were observed. Fairly deep standing water (approximately 1-2 ft) at the junction of sections 1 and 4 with the small ditch (fig. 11) made it impossible to observe the flow discharging from of section 4.

Surface-water flow in the ditches was measured at the same time the water levels were measured in the wells (April 4, 2001), and the locations of these flow measurements are shown in figure 9. The measured flows were 0.23 cubic feet per second (ft^3/s) at location 1 and 0.11 ft^3/s at location 2. Since the flows in the ditches contain water other than ground water, they should be considered an upper limit for ground-water leakage to the storm sewers and ditches. The measured flow at location 2 was lower than at location 1, probably because location 2 had less influence from outside sources of water.

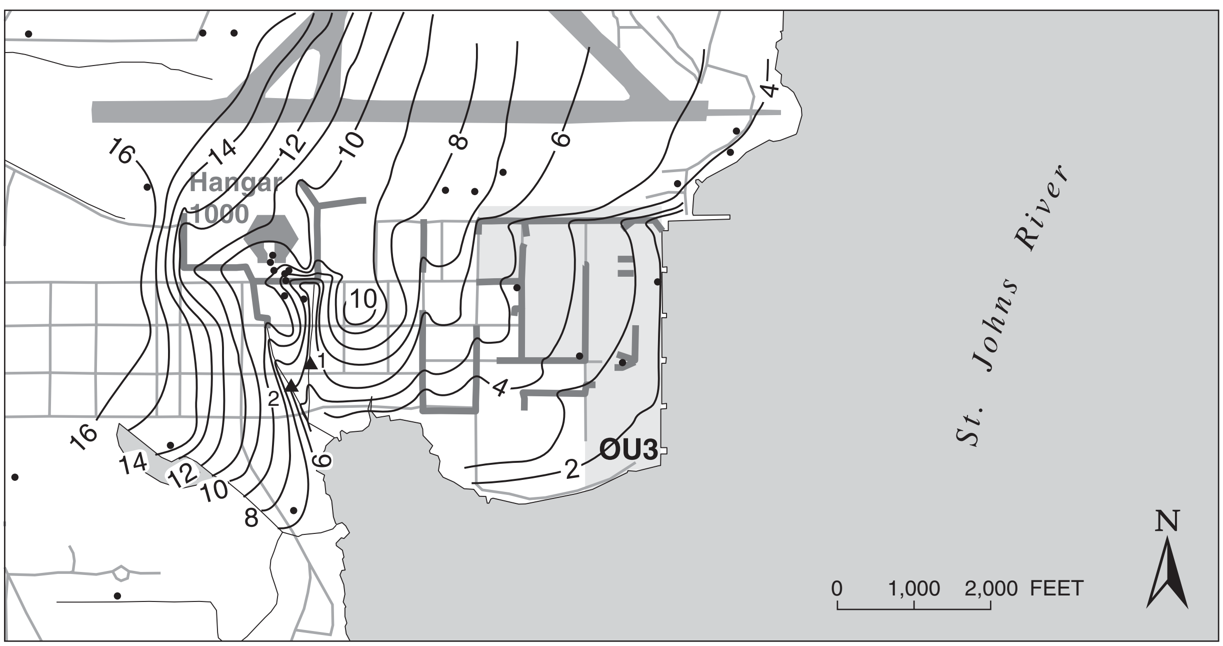

EXPLANATION

— 2 — WATER-TABLE CONTOUR–Shows level to which water would have stood in tightly cased wells tapping the upper layer of the surficial aquifer. Contour interval 1 foot. Datum is NGVD of 1929

STORMWATER DRAINS THAT MAY BE DRAINING GROUND WATER–From the upper layer of the surficial aquifer

• MONITORING WELL LOCATION

1 ▲ SURFACE-WATER MEASUREMENT LOCATION

Figure 9. Water-table surface for the upper layer of the surficial aquifer on April 4, 2001.

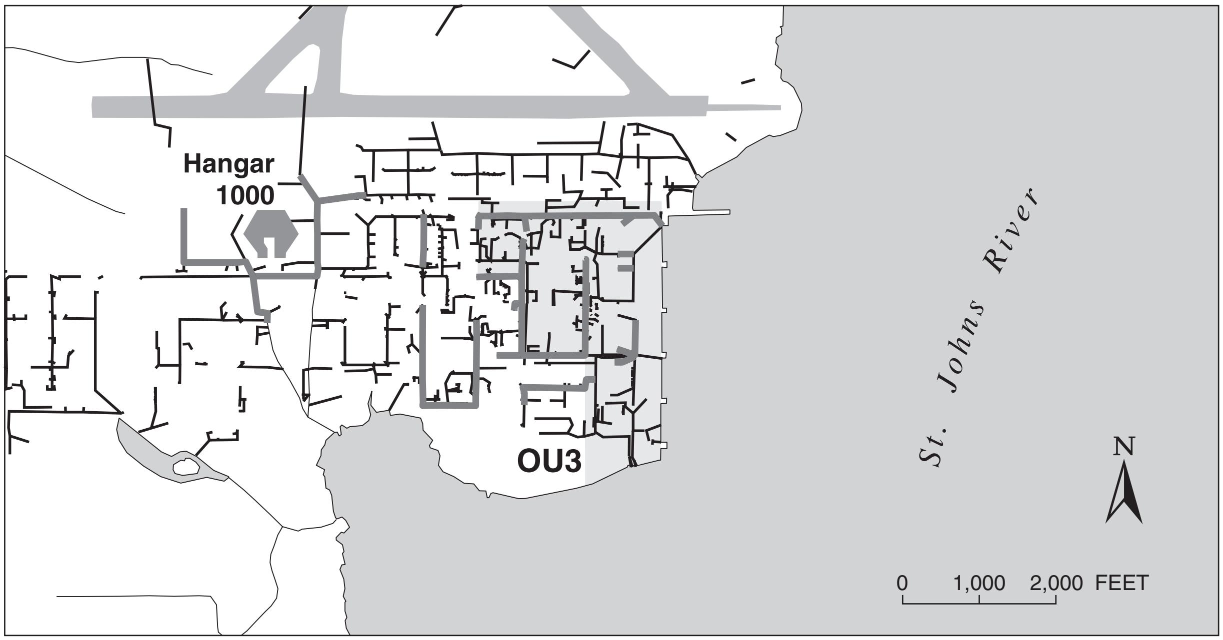

EXPLANATION

STORMWATER DRAINS THAT ARE NOT DRAINING GROUND WATER–From the upper layer of the surficial aquifer

STORMWATER DRAINS THAT ARE DRAINING GROUND WATER–From the upper layer of the surficial aquifer

Figure 10. Stormwater-drainage system at the Jacksonville Naval Air Station.

An attempt was made to measure the flow in sewer section 4 at several locations. At manhole locations 1 and 2 (fig. 11), the flow was not deep enough to submerge a pygmy meter, and the presence of rocks and debris made measurement impossible even though flow was observed. At the sewer outfall location 3 (fig. 11, where sections 1, 4, and the small ditch meet) water was 1-2 ft deep and the velocity was too low to measure.

The potentiometric surface of the intermediate layer shows that ground-water flow is generally eastward toward the St. Johns River (fig. 13). The eastward movement of ground water is partially redirected southward by clay deposits underlying OU3. The horizontal and vertical distribution of this clay deposit is based on extensive drilling at OU3 by Navy consultants (U.S. Navy, 1998); additional discussion of the clay and its effect on ground-water flow was documented in ground-water modeling studies by Davis (1998; 2000).

The surficial aquifer is not used for water supply at the Station or surrounding areas, so ground-water level fluctuations are due to natural variations in recharge, evapotranspiration, and discharge to creeks and rivers. Water-level fluctuations in the surficial aquifer from 1993 to 2001 are shown in figure 14. As shown in the figure, water levels fluctuate seasonally but show no long-term trend. No systematic collection of water-level data has occurred since 1997. Only well MW-45 has had a recent water-level measurement and that was taken on April 4, 2001. This measurement was at the low end of the previously observed range but was taken during an extended period of low rainfall. Since water levels at the Station show no long-term trends, the system could be analyzed assuming steady-state conditions.

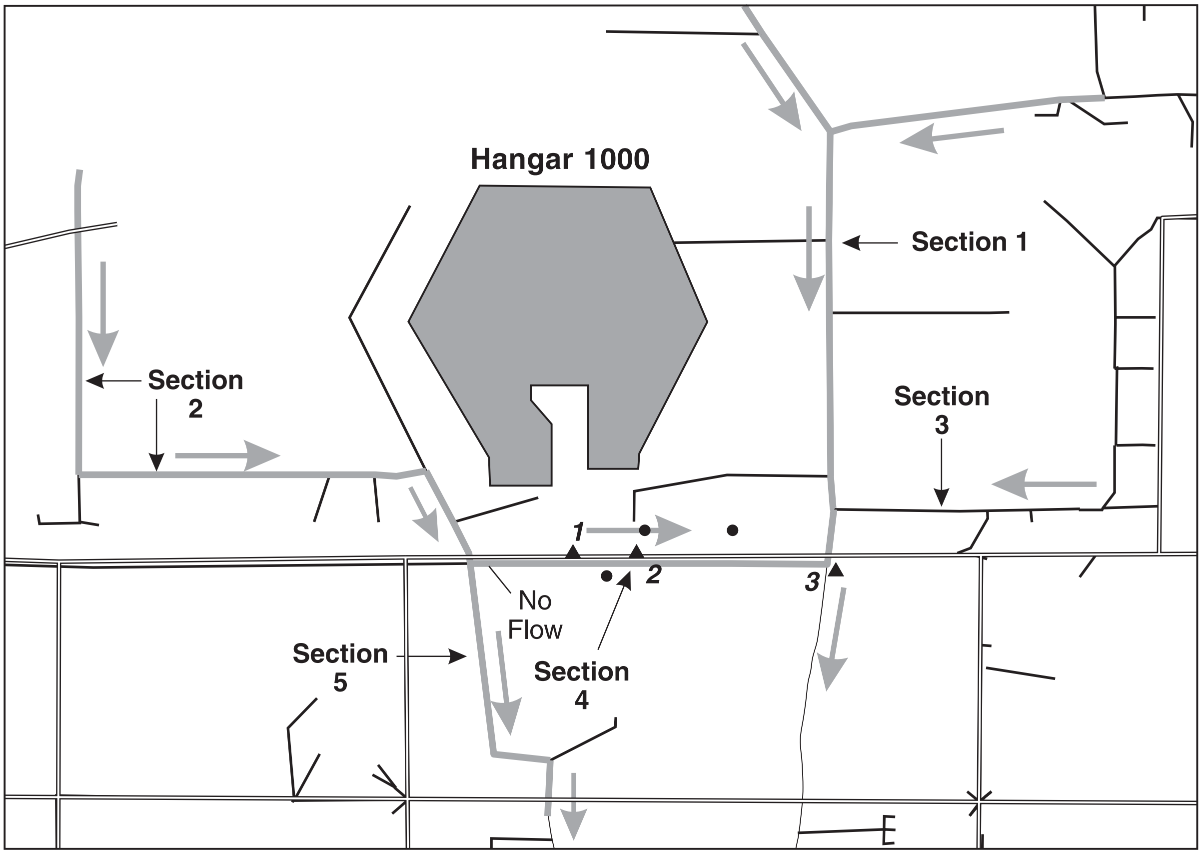

EXPLANATION

STORMWATER DRAINS THAT ARE NOT DRAINING GROUND WATER–From the upper layer of the surficial aquifer

STORMWATER DRAINS THAT ARE DRAINING GROUND WATER–From the upper layer of the surficial aquifer

DIRECTION OF WATER FLOW–In storm drain or ditch

1 ▲ STORM SEWER SAMPLING LOCATION–Locations 1 and 2 are at manholes, location 3 is at the storm sewer outfall

● SAMPLING LOCATION FOR TOTAL ORGANIC CARBON

Figure 11. Location of sewer sections in the vicinity of Hangar 1000.

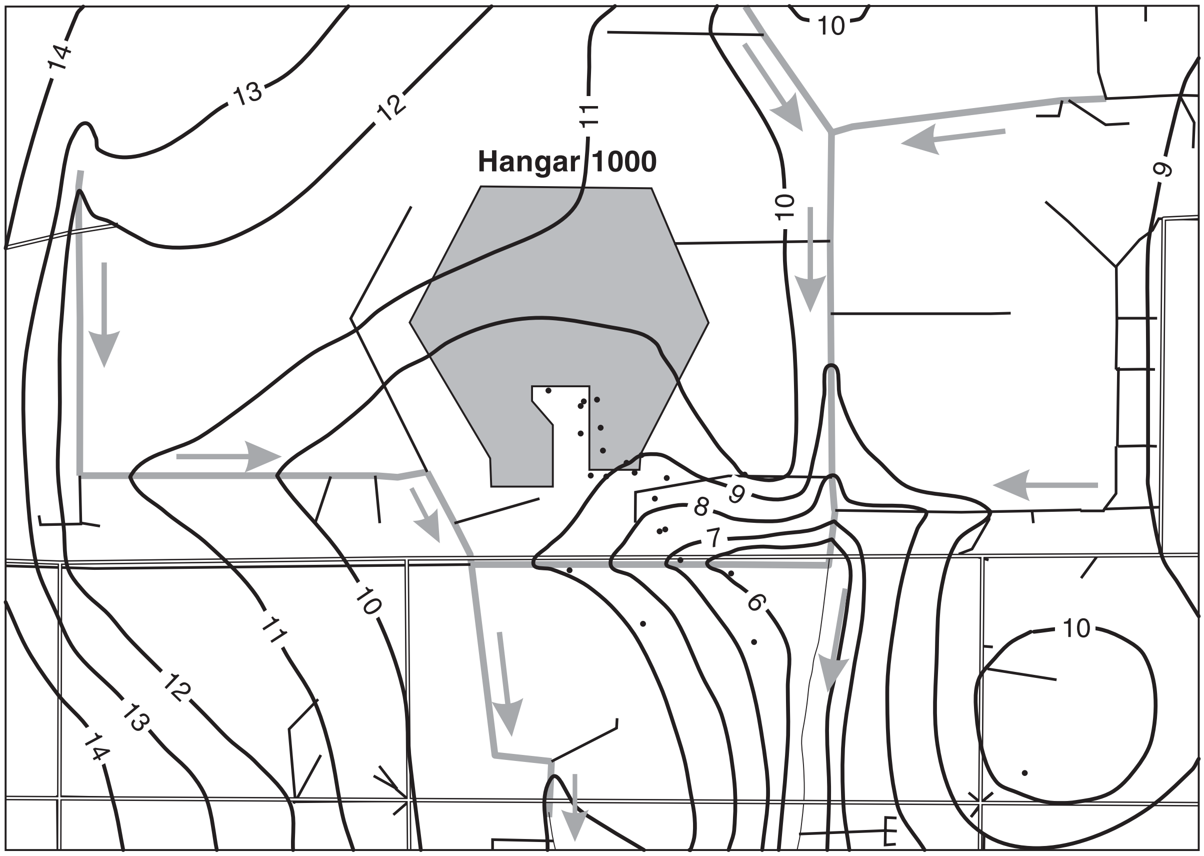

EXPLANATION

— 10 — WATER-TABLE SURFACE CONTOUR–Showing the surface of the water table in feet above NGVD of 1929. Contour interval is 1 foot

STORMWATER DRAINS THAT ARE NOT DRAINING GROUND WATER–From the upper layer of the surficial aquifer

STORMWATER DRAINS THAT ARE DRAINING GROUND WATER–From the upper layer of the surficial aquifer

DIRECTION OF WATER FLOW–In storm drain or ditch

• MONITORING WELL LOCATION

Figure 12. Water-table surface for the upper layer of the surficial aquifer on April 4, 2001, in the vicinity of Hangar 1000.

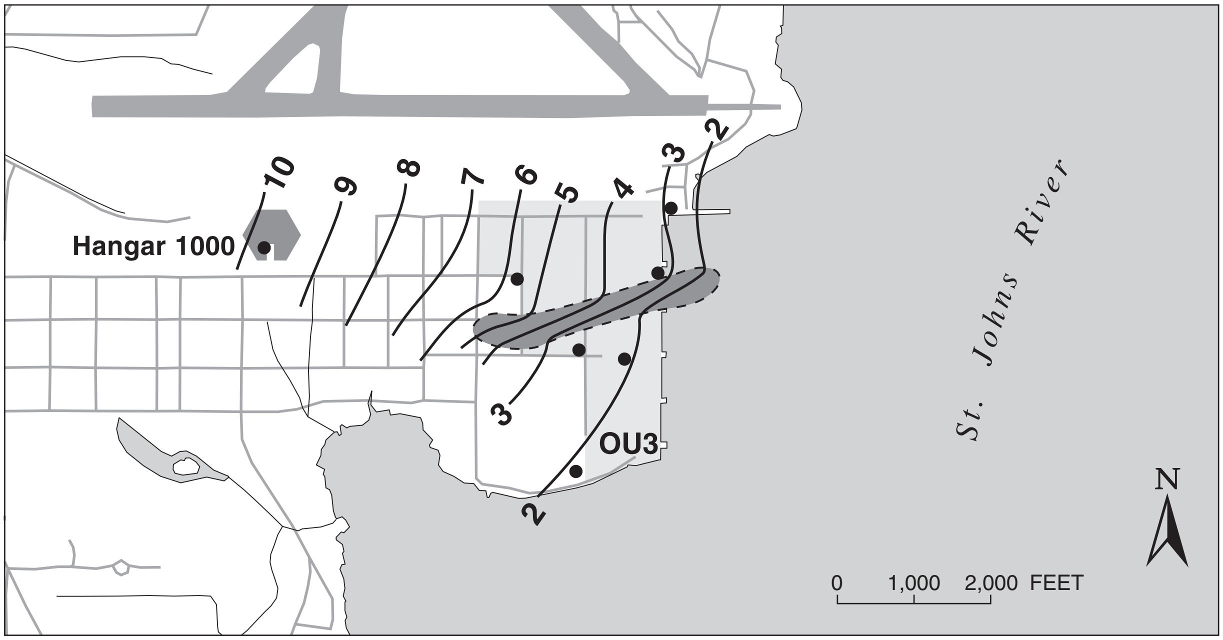

EXPLANATION

CLAY DEPOSITS

—2— POTENTIOMETRIC CONTOUR–Shows level to which water would have stood in tightly cased wells tapping the intermediate layer of the surficial aquifer. Contour interval 1 foot. Datum is NGVD of 1929

● MONITORING WELL LOCATION

Figure 13. Potentiometric surface for the intermediate layer of the surficial aquifer on April 4, 2001.

OCCURRENCE AND FACTORS AFFECTING THE MOVEMENT OF TRICHLOROETHENE, DICHLOROETHENE, AND VINYL CHLORIDE

The ground-water contaminants of concern at Hangar 1000 are TCE, DCE, and VC. The present distribution of these chemicals in the ground water, and the factors affecting their future movement are discussed in this section. The current extent of the contaminant plumes is based on data collected by Tetra Tech and is more fully discussed in Navy documentation on Hanger 1000 (U.S. Navy, written commun., 2002). The location of monitoring wells used to define the plumes is shown in figure 15.

TCE, DCE, and VC are known to degrade in natural environments due to reductive dehalogenation (Zheng and Bennett, 1995). TCE degrades to DCE which degrades to VC, which can further degrade to ethene. Degradation occurs when a chlorine molecule is removed and replaced by a hydrogen molecule. The rate of degradation can be extremely variable even over small distances and depends on the particular compound and the micro-environments within the aquifer. Conditions at Hangar 1000 are generally favorable for anaerobic processes due to several reduction pathways including iron reduction, sulfate reduction, and methanogenesis (U.S. Navy, in press).

The distribution of TCE in the ground water at Hangar 1000 is shown in figure 16. All of the contamination associated with the previously removed storage tanks is located in the upper layer of the surficial aquifer. The highest concentration of TCE, 8,710 µg/L, was measured in a well installed in the location where the TCE storage tanks had been removed suggesting that free product is present because of the high levels. The TCE is migrating from the source area toward storm sewer section 4. As discussed earlier, ground water is leaking into the storm sewer in this area, so it is likely that the sewer is the discharge point for the contaminated ground water; TCE was not detected in monitoring wells south of the storm sewer.

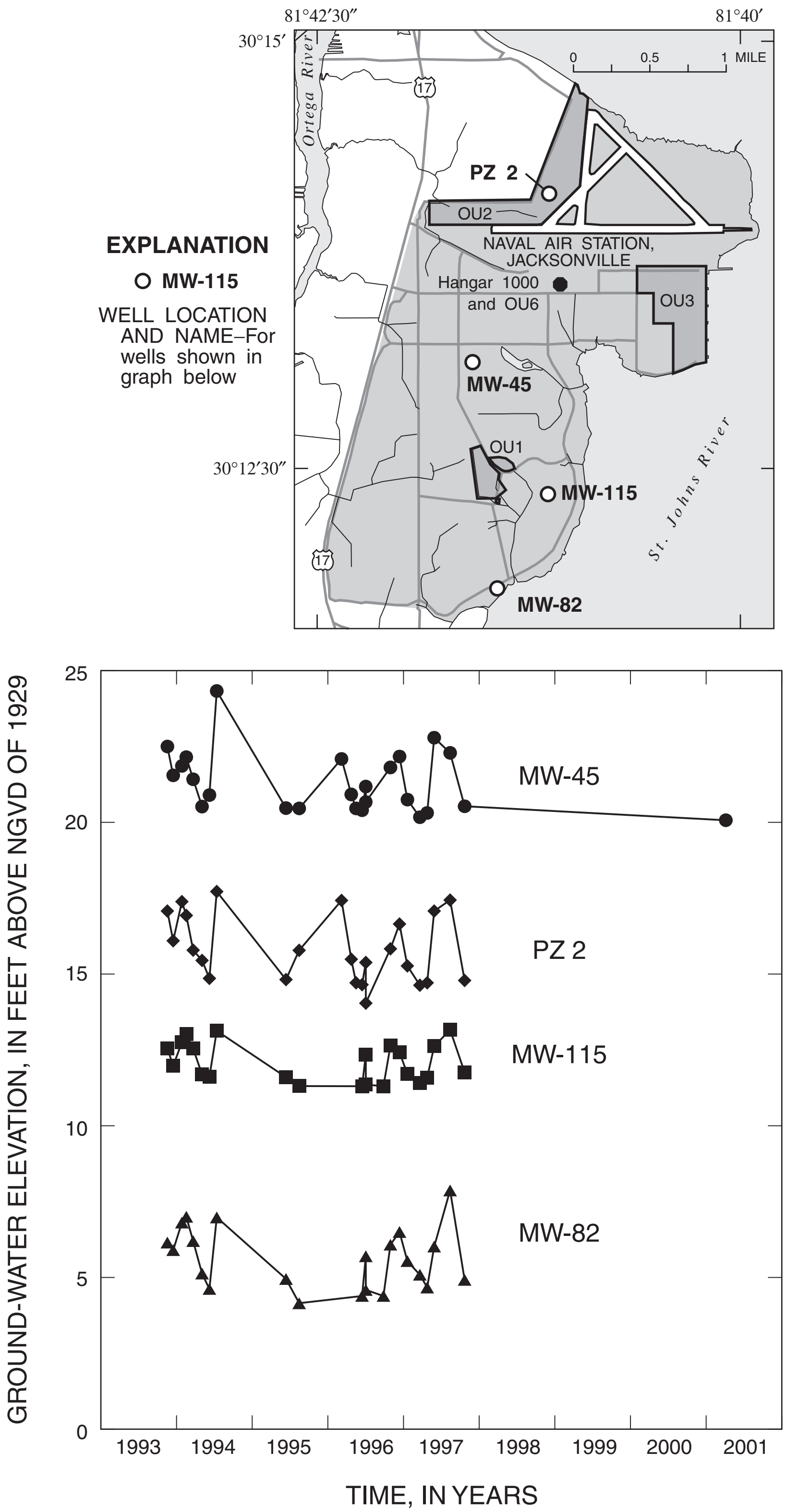

Figure 14. Water-level fluctuations in the surficial aquifer from 1993 to 2001.

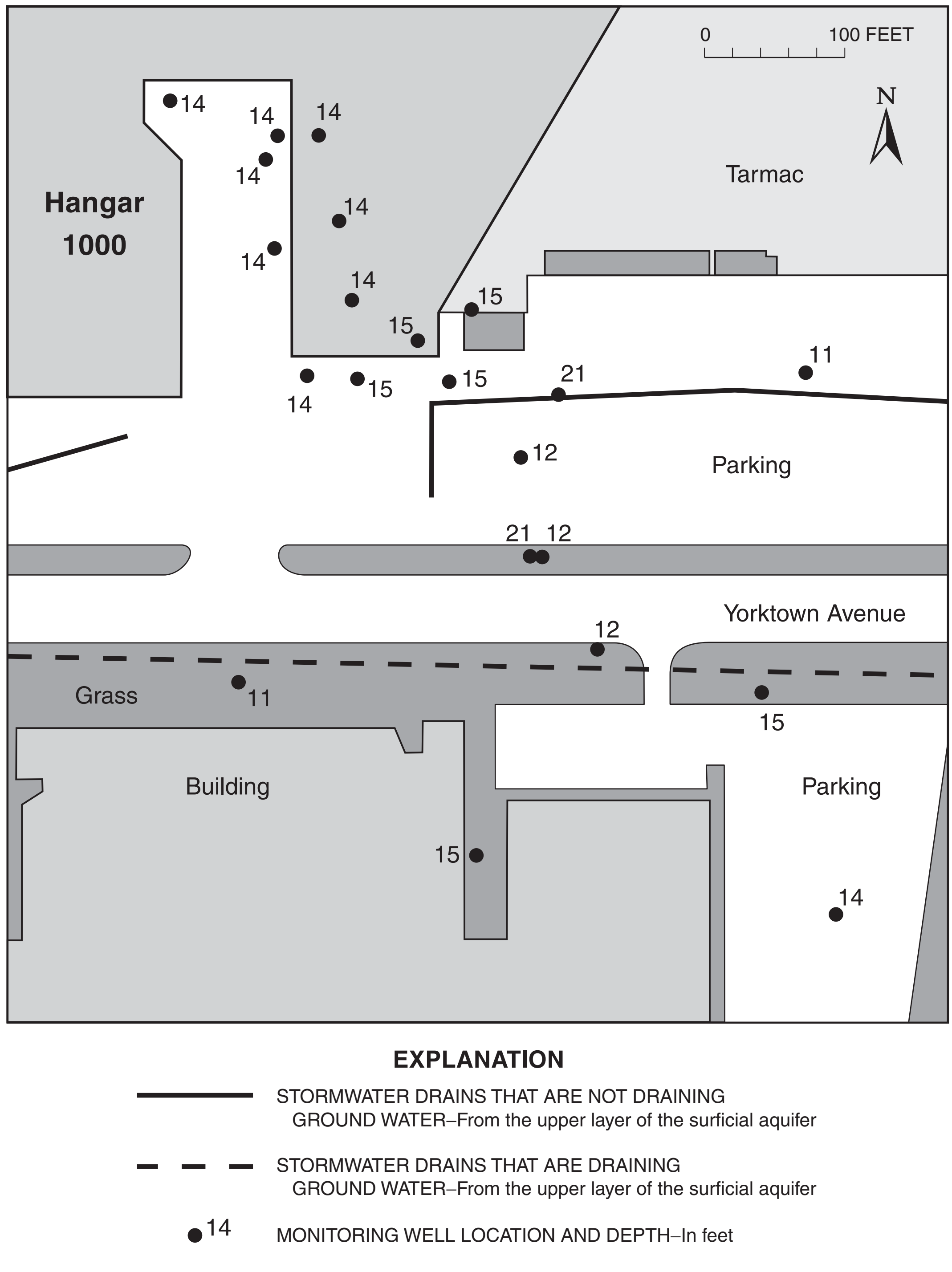

Figure 15. Location of wells where ground-water quality samples were collected.

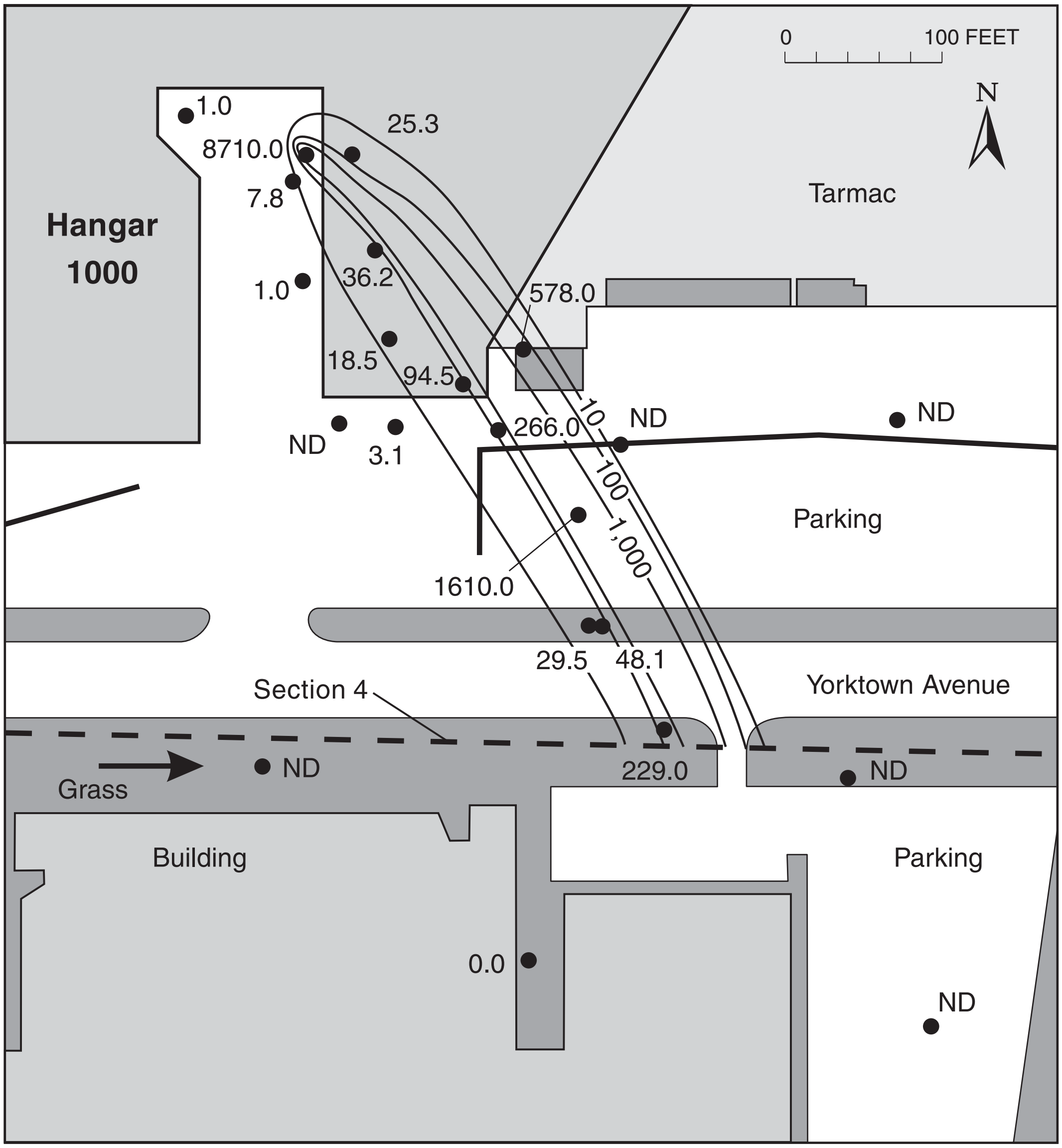

EXPLANATION

—10— LINE OF EQUAL CONCENTRATION OF TRICHLOROETHENE (TCE)–In micrograms per liter. Contour interval is variable

STORMWATER DRAINS THAT ARE NOT DRAINING GROUND WATER–From the upper layer of the surficial aquifer

STORMWATER DRAINS THAT ARE DRAINING GROUND WATER–From the upper layer of the surficial aquifer

● 1.0 MONITORING WELL LOCATION AND TCE CONCENTRATION–In micrograms per liter. "ND" indicates no detection

DIRECTION OF WATER FLOW–In storm drain or ditch

Figure 16. Distribution of trichloroethene (TCE) contamination in the ground water of the surficial aquifer at Hangar 1000 on January 17, 2001.

Tetra Tech sampled the water flowing in the storm sewer at the three locations shown in figure 11. No TCE was detected in any of these samples. This would be expected in locations 1 and 2 because they are upstream of the area where contaminated water would be expected to discharge to the storm sewer, but not in location 3. If the sewer is receiving the contaminated ground water, then the lack of detection at location 3 could be the result of several factors. First, videos taken in the storm sewers at OU3 showed that water entering the sewers at joints and cracks commonly runs down the pipes as film flow, thus allowing a substantial amount of volatilization. Second, the flow in the sewer pipe is small and essentially sheet flow, thus allowing more volatilization. Third, dilution in the standing water at the sewer outfall is occurring due to flow that can be observed coming from the sewer to the north.

If the contaminated ground water is passing beneath the sewer, then it would probably discharge directly to the small ditch to the southeast. However, no contaminants have been detected in the monitoring wells south of sewer section 4.

The distribution of DCE in the ground water is shown in figure 17. The source of DCE contamination is probably the result of reductive dehalogenation of TCE and leakage from the tanks. Concentrations of DCE at Hangar 1000 are roughly the same as that of TCE. The distribution of VC in ground water is shown in figure 18. Concentrations of VC are low, indicating either that the dehalogenation of DCE to VC is occurring relatively slowly or more likely that the destruction of VC is occurring relatively rapidly.

Contaminants dissolved in ground water will move by advection in the direction of flow. However, other natural processes can modify the movement of contaminants, causing the concentrations to change or causing contaminants to move at different rates than the ground water. Major processes affecting contaminant movement are advection, hydrodynamic dispersion, biodegradation, and retardation due to sorption to the sediments.

The most important factor affecting contaminant movement is advection, which is the transport of dissolved constituents with the velocity and direction of ground-water flow. Most of the surficial ground water (containing the contaminants) at Hangar 1000 probably discharges to the storm drains, which then discharges to a small creek that flows to the St. Johns River.

Hydrodynamic dispersion occurs due to the mechanical mixing of moving ground water and molecular diffusion of the dissolved chemical. Dispersion will cause a contaminant plume to spread, resulting in lower solute concentrations away from the plume center. Dispersion is usually difficult to accurately quantify in the field. Gelhar and others (1992) performed a critical review of field-scale dispersion studies to define reasonable dispersivity values. Using data that Gelhar and others (1992) described as the most reliable, a high value for longitudinal dispersivity (in the direction of the flow axis) was 5.6 ft for sites similar to Hangar 1000 and a low value was 0.98 ft. A high value for transverse dispersivity (perpendicular to the flow axis) was 0.30 ft and a low value was 0.033 ft. When simulating solute movement, low values of dispersivity will result in the highest predicted concentrations.

The rate of movement of a dissolved chemical depends on the ground-water flow velocity and the retardation factor of the particular chemical. The retardation factor is the ratio of the velocity of ground water to the velocity of the chemical. For example, a retardation factor of 1.5 means that ground water moves 1.5 times faster than the dissolved chemical. Retardation of TCE, DCE, and VC occurs because these chemicals are nonpolar, which causes them to partition to the organic matter in the aquifer sediments. Therefore, retardation and retardation factors are a function of the fraction of organic carbon content (f_{oc}) of the aquifer. Partitioning is a reversible process; molecules that have partitioned to the organic matter will move back into the ground water as relative concentrations change.

The organic carbon content in the upper layer of the surficial aquifer at Hangar 1000 was measured at three locations (fig. 11). The measured values were of 1,200 $\text{milligrams}_{\text{organic carbon}}$ per $\text{kilograms}_{\text{soil}}$ (mg_{oc}/kg_{soil}), 1,200 mg_{oc}/kg_{soil} and 3,280 mg_{oc}/kg_{soil}. The average of these is 1,893 mg_{oc}/kg_{soil} or an average f_{oc} of 1.893×10^{-3} mg_{oc}/kg_{soil} (the f_{oc} is calculated by dividing the organic carbon content by 1,000,000). The distribution coefficient (K_d) relates the mass of contaminant dissolved in the ground water to the mass sorbed to the sediments.

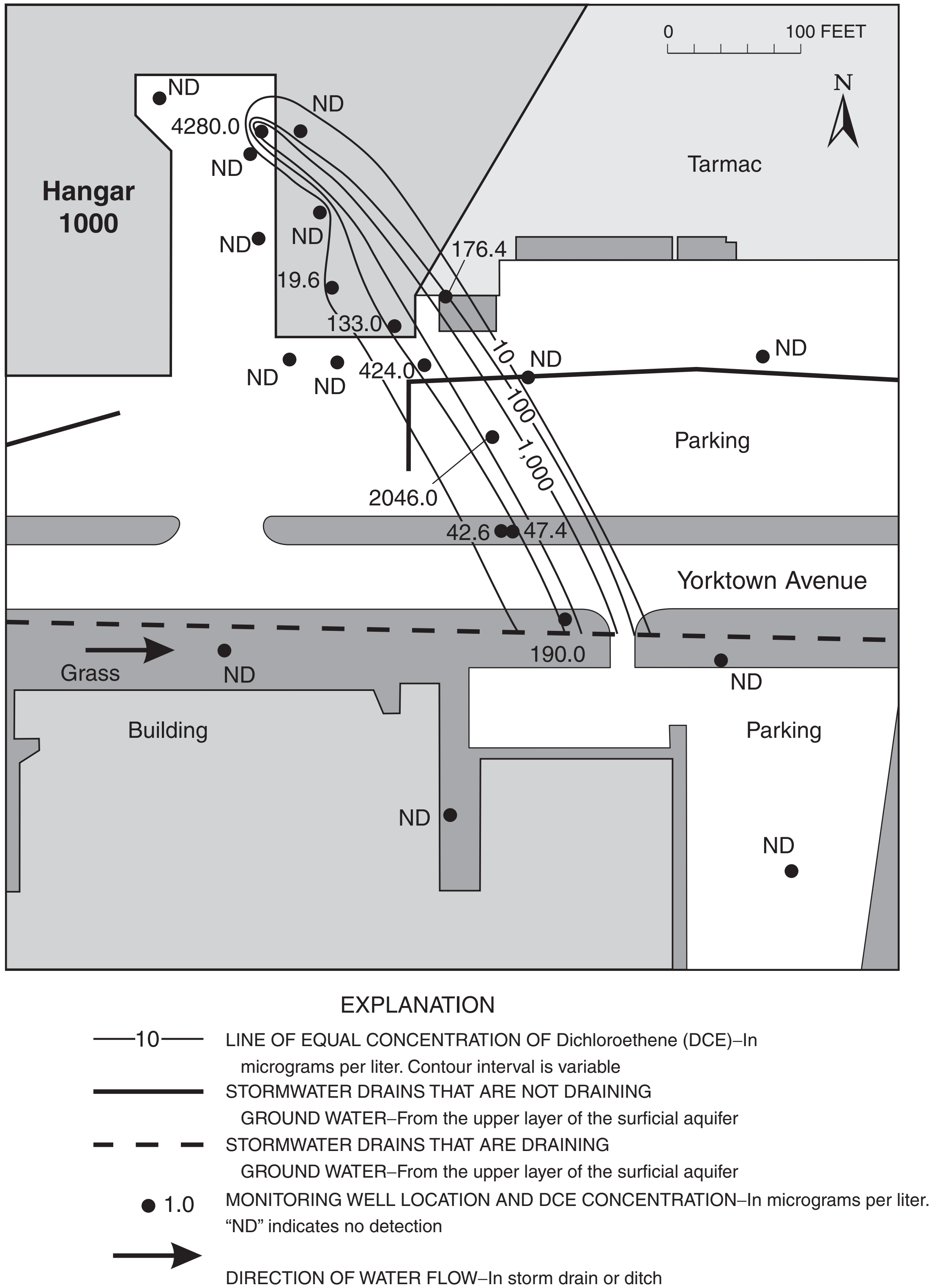

Figure 17. Distribution of dichloroethene (DCE) contamination in the ground water of the surficial aquifer at Hangar 1000 on January 17, 2001.

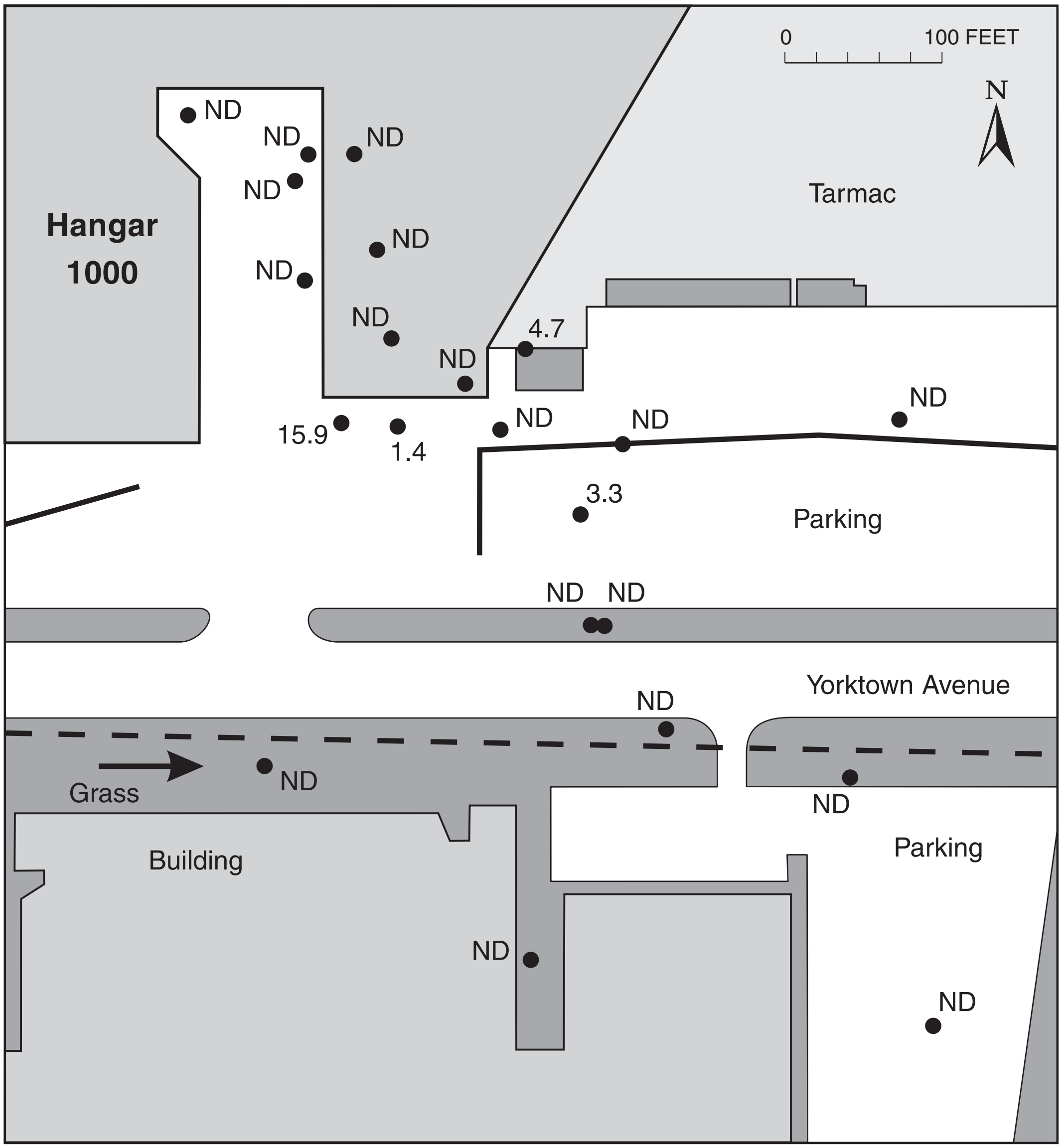

EXPLANATION

STORMWATER DRAINS THAT ARE NOT DRAINING GROUND WATER–From the upper layer of the surficial aquifer

STORMWATER DRAINS THAT ARE DRAINING GROUND WATER–From the upper layer of the surficial aquifer

1.4 MONITORING WELL LOCATION AND VINYL CHLORIDE (VC) CONCENTRATION–In micrograms per liter. “ND” indicates no detection

DIRECTION OF WATER FLOW–In storm drain or ditch

Figure 18. Distribution of vinyl chloride (VC) contamination in the ground water of the surficial aquifer at Hangar 1000 on January 17, 2001.

Partitioning coefficients were calculated using the following equation with resulting values given in table 3:

$$K_d = K_{oc}f_{oc} ,$$

where

K_d = distribution coefficient, milliliters water per grams_{soil} (mL_{water}/g_{soil}),

K_{oc} = partition coefficient, mL_{water}/g_{oc}, and

f_{oc} = fraction organic carbon, in $\text{grams}_{\text{organic carbon}}$ per grams_{soil} (g_{oc}/g_{soil}).

The retardation factor for the upper layer was calculated using the following equation, with the results given in table 3. Reasonable values for bulk density of 1.6 grams per cubic centimeter (g/cm^3) and total porosity of 25 percent (Hillel, 1980) were assumed for the aquifer sediments.

$$R = 1 + \frac{(\rho)(K_d)}{\phi} ,$$

where

R = retardation factor, no units,

ρ = bulk density of aquifer material, in g/cm^3,

K_d = distribution coefficient, mL_{water}/g_{soil}, and

ϕ = aquifer porosity, $\text{milliliters}_{water}$ per cubic centimeter_{soil} (mL_{water}/cm^3_{soil}).

Table 3. Distribution of partitioning coefficients and retardation factors for trichloroethene (TCE), dichloroethene (DCE), and vinyl chloride (VC) for the upper layer of the surficial aquifer

[f_{oc}, fraction organic carbon; mL_{water}, milliliters water; g_{soil}, grams soil; K_{oc}, partition coefficient; g_{oc}, grams organic carbon; K_d, distribution coefficient]

	TCE	DCE	VC
Average f_{oc} (mL_{water}/g_{soil})	1.893×10^{-3}	1.893×10^{-3}	1.893×10^{-3}
K_{oc} (mL_{water}/g_{oc})	126[a]	86[a]	57[a]
K_d (mL_{water}/g_{soil})	0.2386	0.1628	0.1079
Retardation factor (no units)	2.5	2.0	1.7

[a] Mercer and others, 1990.

GROUND-WATER FLOW SIMULATION AT THE STATION

Several ground-water flow models have been developed, each designed to satisfy a particular need of the Station. Because of the contaminant plumes of TCE, DCE, and VC identified in the area of Hangar 1000, a model was needed to simulate the contaminant concentration and movement of these chemicals. Before solute transport modeling could be performed, ground-water flow had to be simulated. This section discusses the simulation of ground-water flow and the next section discusses the solute transport modeling at Hangar 1000.

Original Subregional Model

The original subregional OU3 model (Davis, 1998) was calibrated to the head data collected on October 29 and 30, 1996, and steady-state ground-water flow conditions were assumed. The calibration strategy was to match simulated heads in the upper and intermediate layers to within 1 ft of the measured values. After calibration, all of the model simulated heads matched the measured heads within the calibration criterion of 1 ft, and 48 of 67 simulated heads (72 percent) were within 0.5 ft of the corresponding measured values.

The original model contained 78 rows and 148 columns of active model cells; all cells were 100 ft on each side. Vertically, the surficial aquifer was divided into two layers. The upper model layer represented the upper layer of the surficial aquifer and extended from land surface down to 15 ft below sea level (sea level refers to the National Geodetic Vertical Datum of 1929 (NGVD29)); this layer was modeled as unconfined. The lower model layer represented the intermediate layer and extended from the bottom of the upper layer down to the top of the Hawthorn Group; this layer was modeled as confined. The clay layer separating the upper and intermediate layers was simulated through the vertical leakance term. A seawall at OU3 was simulated using the Horizontal-Flow Barrier Package documented by Hseih and Freckleton (1993).

The northern, western, and southern boundaries of the model were simulated as no flow and were positioned along ground-water divides delineated using both water-table maps and particle tracking with the regional model (fig. 2). The eastern model boundary also is no-flow and is positioned near the center of the

St. Johns River. This boundary was positioned away from the shoreline so that the model could simulate the upward seepage of ground water through the bottom of the river. The base of the surficial aquifer was simulated as a no-flow boundary because it is underlain by the low-permeability sediments of the Hawthorn Group. There is little, if any, vertical flow between the surficial aquifer and the Hawthorn Group.

The MODFLOW River Package was used to simulate, in the upper layer of the model, the presence of the St. Johns River and two small ditches. The riverbed conductance for the St. Johns River was calculated using a riverbed thickness of 1 ft over the entire area of each cell and a riverbed hydraulic conductivity of 8 feet per day (ft/d). The altitude of the bottom of the river was taken from USGS topographic maps and a stage of 1 ft above sea level (NVGD29). Conductance for two small ditches was calculated using a thickness of 1 ft, a width of 10 ft, and a hydraulic conductivity of 4 ft/d. The altitude of the stage and bottom of the two ditches were estimated from the topographic maps and field observations.

The MODFLOW Drain Package was used to simulate the presence of the stormwater drains in the upper model layer. The altitude, relative to the NGVD29, of the bottom of the drains was determined where manholes allowed access. Altitudes between manholes were extrapolated from the measured values.

The distribution of recharge ranged from 13.0 inches per year (in/yr) in irrigated areas to 0.4 in/yr in relatively impervious areas. The horizontal hydraulic conductivity for the upper layer ranged from 0.5 to 7.5 ft/d, while the horizontal hydraulic conductivity in the intermediate layer ranged from 20 ft/d in a sandy area to 0.2 ft/d within the low-permeability silt and clay deposits.

Recalibration of the Subregional Model

The recalibrated model used the same grid location and discretization of 78 rows and 148 columns of active model cells (measuring 100 ft on each side, fig. 19) as the original subregional

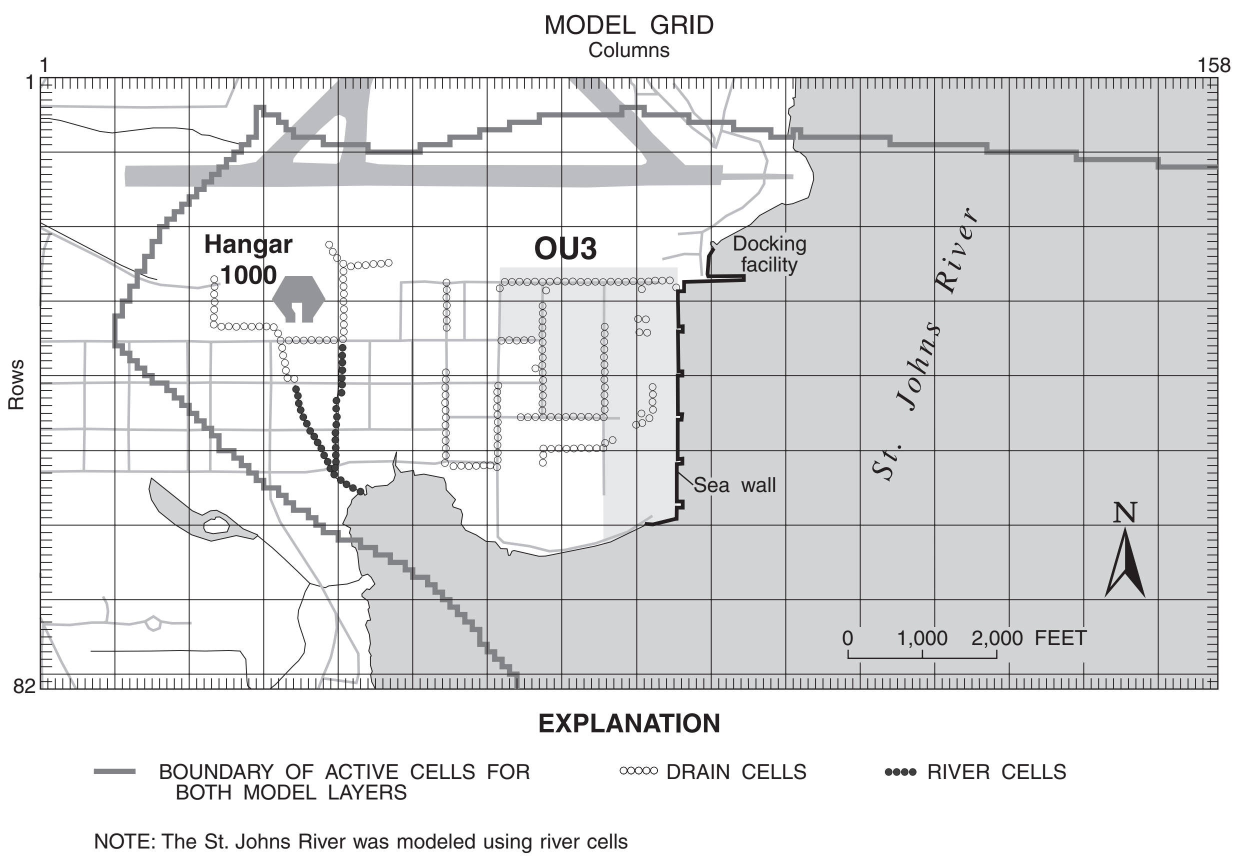

Figure 19. Location and orientation of the subregional model finite-difference grid.

model. The lateral boundaries and extent of the recalibrated model are the same as the original model. The surficial aquifer was divided into four layers (instead of the two layers in the original model) to more accurately simulate the complex hydrology (fig. 20). Layer 1 of the original model was split into layers 1 and 2; layers 3 and 4 are the result of splitting layer 2 of the original model. Model layer 1 represents the upper layer of the surficial aquifer and extends from land surface down to about 15 ft below land surface; this layer was modeled as unconfined. Layer 2 represents most of the clay layer shown in figure 5 (the deeper parts of the clay are simulated in layers 3 and 4). Model layers 3 and 4 represent the intermediate layer of the surficial aquifer and were modeled as confined. The top of the Hawthorn Group forms the base of the surficial aquifer. A seawall, located at OU3, was simulated using the Horizontal-Flow Barrier Package documented by Hseih and Freckleton (1993). The initial aquifer parameters, before recalibration, were all taken directly from the original model. The hydraulic conductivity of the clay layer (which was not explicitly modeled in the original model) was estimated using the vertical conductance and thickness.

The model was calibrated to the head data collected on April 4, 2001. Water levels were collected across the entire northern part of the Station and contoured to verify that the ground-water divides (which established the model boundaries) were the same as for the original model. The relatively thin aquifer and numerous small creeks draining ground water tend to stabilize ground-water levels and the locations of ground-water divides. During recalibration, the following parameters were varied: horizontal and vertical hydraulic conductivities of all layers, the recharge rates, and riverbed conductances. The parameter changes during recalibration were generally minor, so the recalibrated model is similar to the original model.

Steady-state ground-water flow conditions were assumed. The calibration strategy was to match simulated heads in the upper and intermediate layers to within 1.5 ft of the measured values. When calibration was completed, 45 of the 46 model-simulated heads matched the measured heads to within the 1.5-ft calibration criterion, 41of 46 simulated heads (89 percent) were within 1.0 ft, and 27 of 46 simulated heads (59 percent) were within 0.5 ft of the corresponding measured values. Figure 21 shows a comparison of the measured and simulated heads. If the model-simulated heads had matched the measured values exactly, then all the points would lie on the 45 degree line (line of equality).

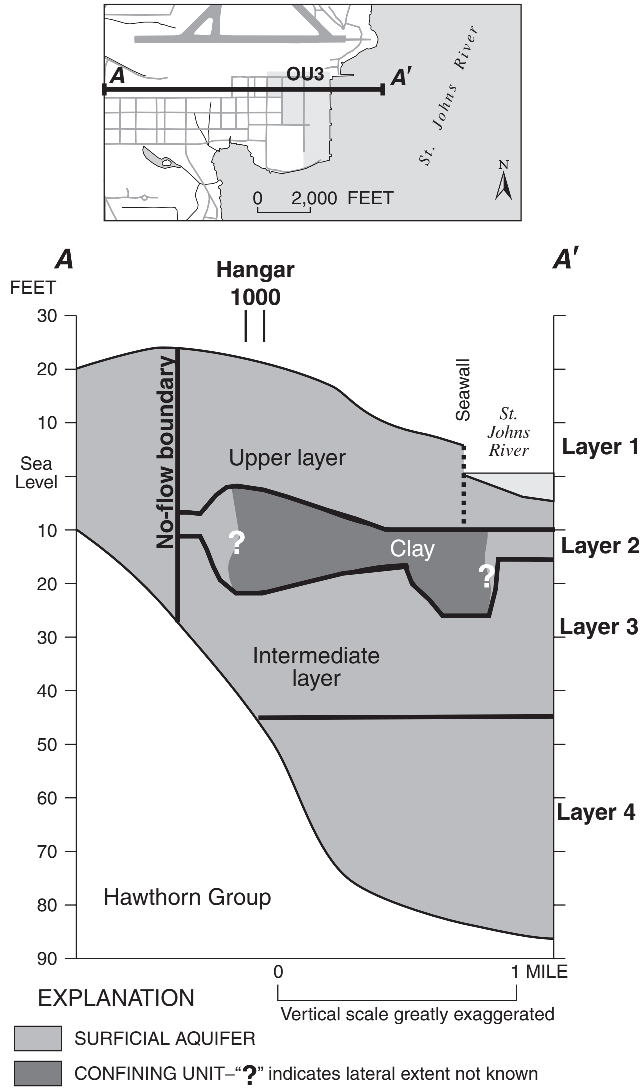

Figure 20. Generalized hydrologic section for the recalibrated subregional model.

The simulated recharge rate for the recalibrated model is shown in figure 22. Recharge ranged from a low of 0.1 in/yr largely in paved areas to 13 in/yr in irrigated areas. Most of the small, irregularly shaped, high recharge areas represent grassy areas within otherwise paved surfaces: the locations of these high recharge areas were determined from aerial photographs. The most significant changes in recharge occured in the grassy areas with higher recharge southeast of Hangar 1000.

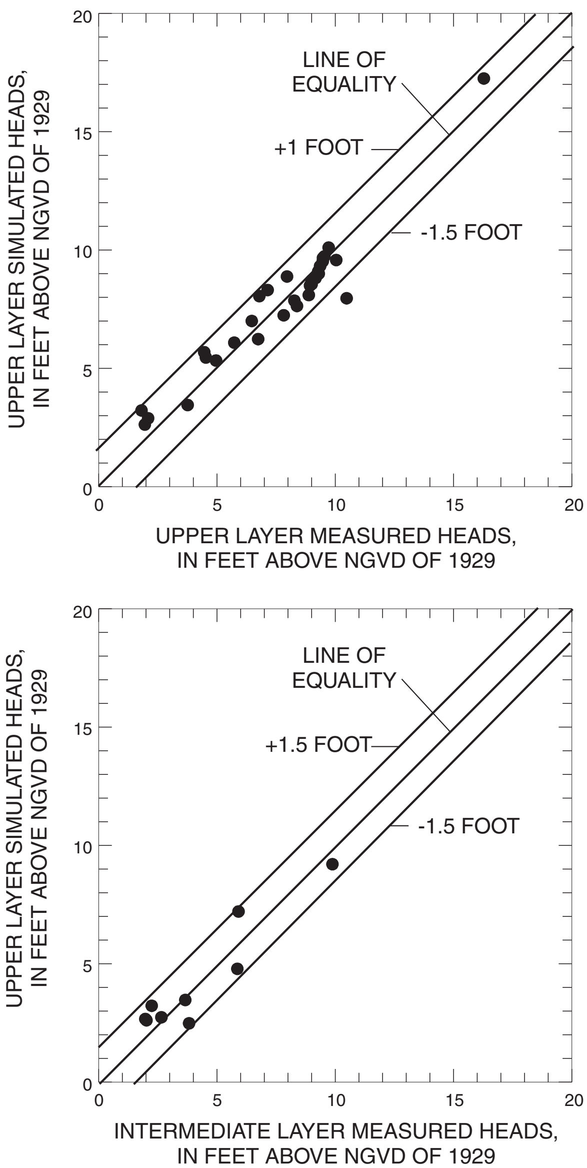

Figure 21. Comparison of measured and simulated heads for the recalibrated subregional model.

The model-simulated horizontal hydraulic conductivity distribution for the upper layer is shown in figure 23. In the central part of the model area, the hydraulic conductivity is 0.5 ft/d, which is very nearly the value of 0.6 ft/d determined from a multiple-well aquifer test (Davis, 1996a,b) conducted at a contaminated site (the test was located approximately at the center of the 0.5-ft/day conductivity area.) The 0.5-ft/d conductivity area has been reduced in size from the original subregional model. The hydraulic conductivity in the southern part of the model area is 1.0 ft/d and was determined during the calibration of the original subregional model. In the remainder of the model area, the simulated hydraulic conductivity was 7.5 ft/d. Aquifer testing of two wells in the upper layer of the surficial aquifer at Hangar 1000 (wells numbered 10 and 19 on figure 7) gave hydraulic conductivities of 4 ft/d and 8 ft/d, respectively (Davis, 2001). The hydraulic conductivity of the surficial aquifer in the original subregional model was 7.5 ft/d; this value was used in the recalibrated model because it gave the best calibration and because it fell between the measured values. The 7.5-ft/d conductivity area has increased in size from the original model. The vertical hydraulic conductivity for this, and all the other layers, is one order of magnitude lower than the horizontal hydraulic conductivity.

The model-simulated horizontal hydraulic conductivity distribution for layer 2 is shown in figure 24. The hydraulic conductivity ranged from a low of 5.0×10^{-6} ft/d in the thicker part of the clay layer to a high of 4.3×10^{-1} ft/d in the area around the old fuel barge dock, where dredging has removed or disturbed the clay. The simulated thickness of layer 2 is shown in figure 25. As seen in the figure, the clay layer is thickest near the center of the model and thins toward the edges.

The model-simulated horizontal hydraulic conductivity distribution for layer 3 is shown in figure 26. The simulated hydraulic conductivity over most of the model area was 7.5 ft/d. The higher 20-ft/d conductivity area at OU3 was based on a multi-well aquifer test (Davis, 1996a,b). The hydraulic conductivity of 0.4 ft/d represents low-permeability silt and clay deposits, and was taken from earlier modeling studies (Davis, 1998). The thickness of layer 3 ranges from 15-20 ft at Hangar 1000 (fig. 27). Near the center of the model, layer 3 thins to about 5 ft, which is due to the thickening of the overlying clay represented by layer 2.

The model-simulated horizontal hydraulic conductivity distribution for layer 4 is shown in figure 28. The distribution is the same as for layer 3 and for the same reasons, except that layer 4 does not extend as far westward as layer 3. The simulated thickness of layer 4 is shown in figure 29. The increase in thickness from west to east is a result of the thinning of the top of the Hawthorn Group which forms the base of layer 4.

The riverbed conductance for the St. Johns River was 8 square feet per day (ft^2/d), except in the area of the docking facility where the conductance was 60 ft^2/d to reflect the disturbance and removal of riverbed sediments during dredging. The conductance of the small ditches was of 4 ft^2/d.

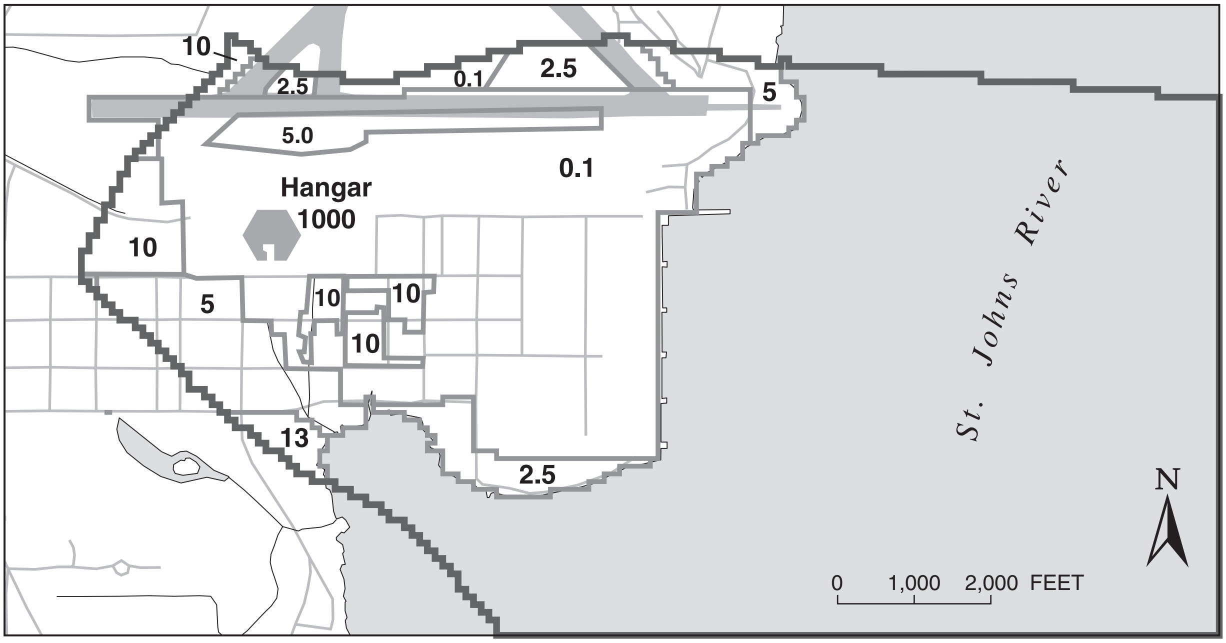

EXPLANATION

SUBREGIONAL STUDY AREA AND SUBREGIONAL MODEL BOUNDARY

BOUNDARY OF RECHARGE ZONES IN MODEL

2.5 RECHARGE RATES–Model simulated, values in inches per year

Figure 22. Simulated recharge rates for the recalibrated subregional model.

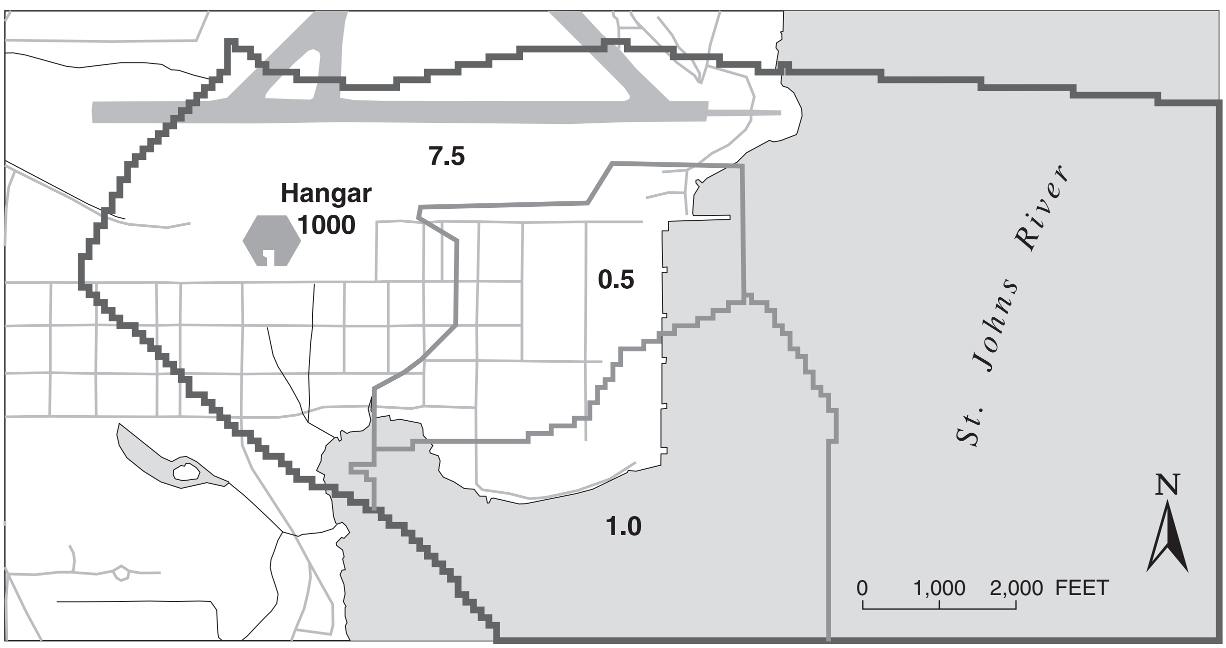

EXPLANATION

SUBREGIONAL STUDY AREA AND SUBREGIONAL MODEL BOUNDARY

BOUNDARY OF MODEL-SIMULATED HORIZONTAL HYDRAULIC CONDUCTIVITY–In the upper layer

1.0 MODEL-SIMULATED HORIZONTAL HYDRAULIC CONDUCTIVITY–In the upper layer, in feet per day

Figure 23. Simulated horizontal hydraulic conductivity of the upper layer of the recalibrated subregional model.

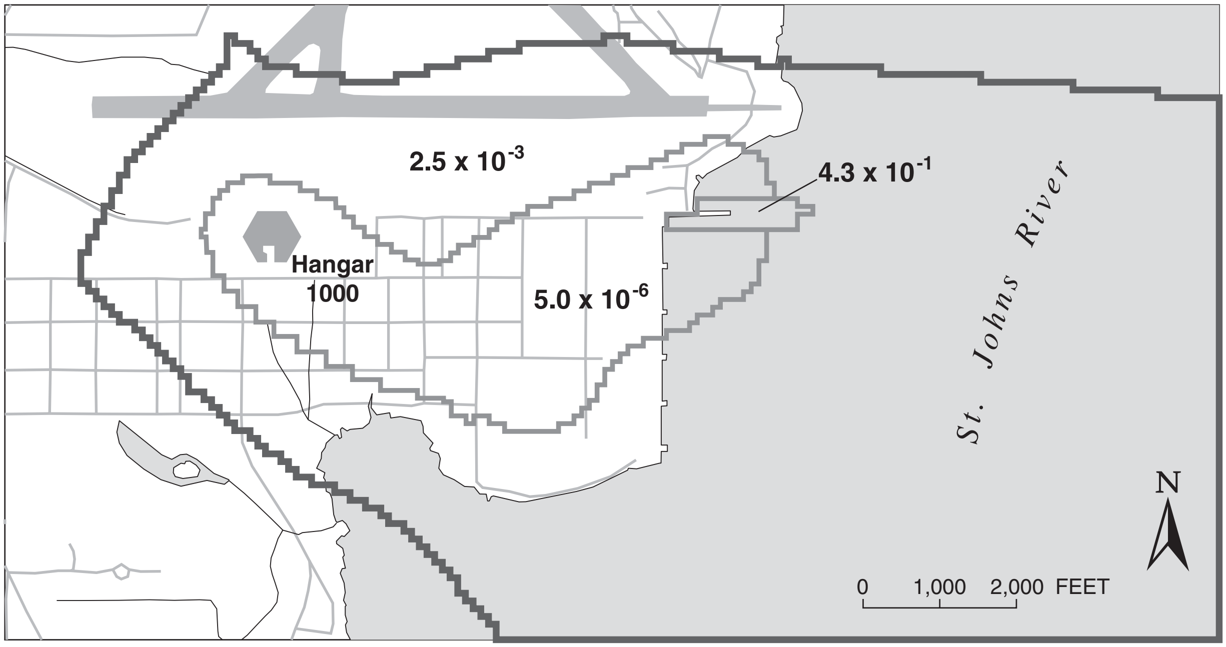

EXPLANATION

SUBREGIONAL STUDY AREA AND SUBREGIONAL MODEL BOUNDARY

BOUNDARY OF MODEL-SIMULATED HORIZONTAL HYDRAULIC CONDUCTIVITY–Of layer 2

2.5×10^{-3} MODEL-SIMULATED HORIZONTAL HYDRAULIC CONDUCTIVITY–Of layer 2, in feet per day

Figure 24. Simulated horizontal hydraulic conductivity of layer 2 of the recalibrated subregional model.

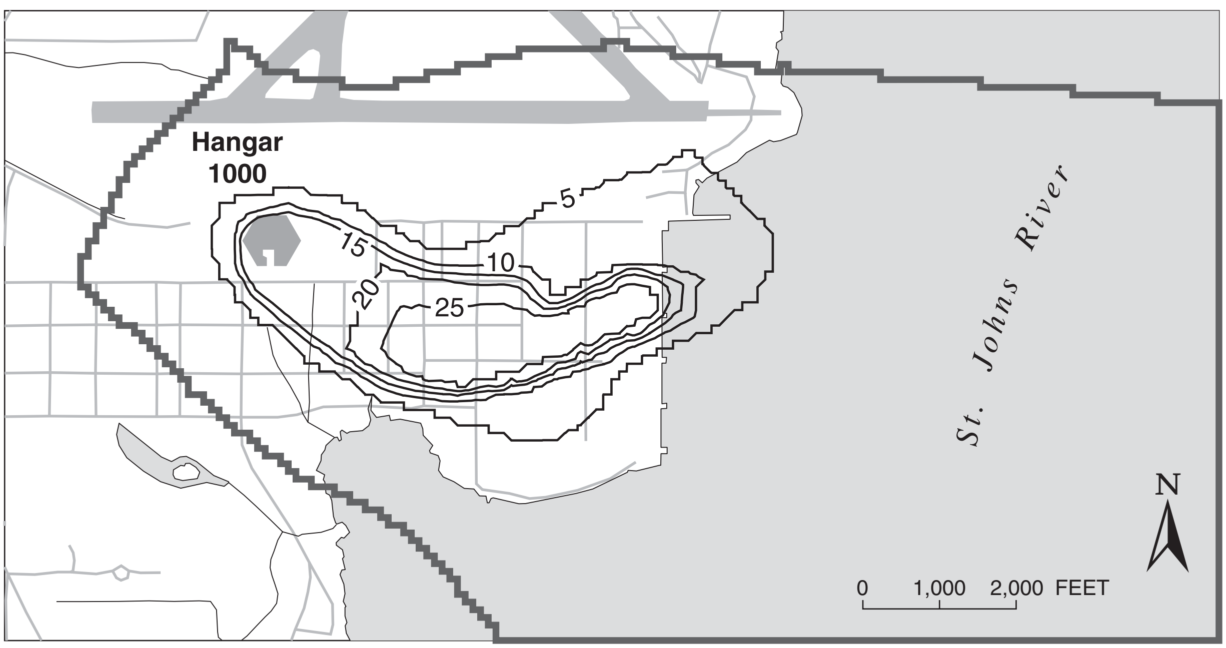

EXPLANATION

SUBREGIONAL STUDY AREA AND SUBREGIONAL MODEL BOUNDARY

20 LINE OF EQUAL SIMULATED THICKNESS OF LAYER 2–Of the subregional model, in feet.

Figure 25. Simulated thickness of layer 2 of the recalibrated subregional model.

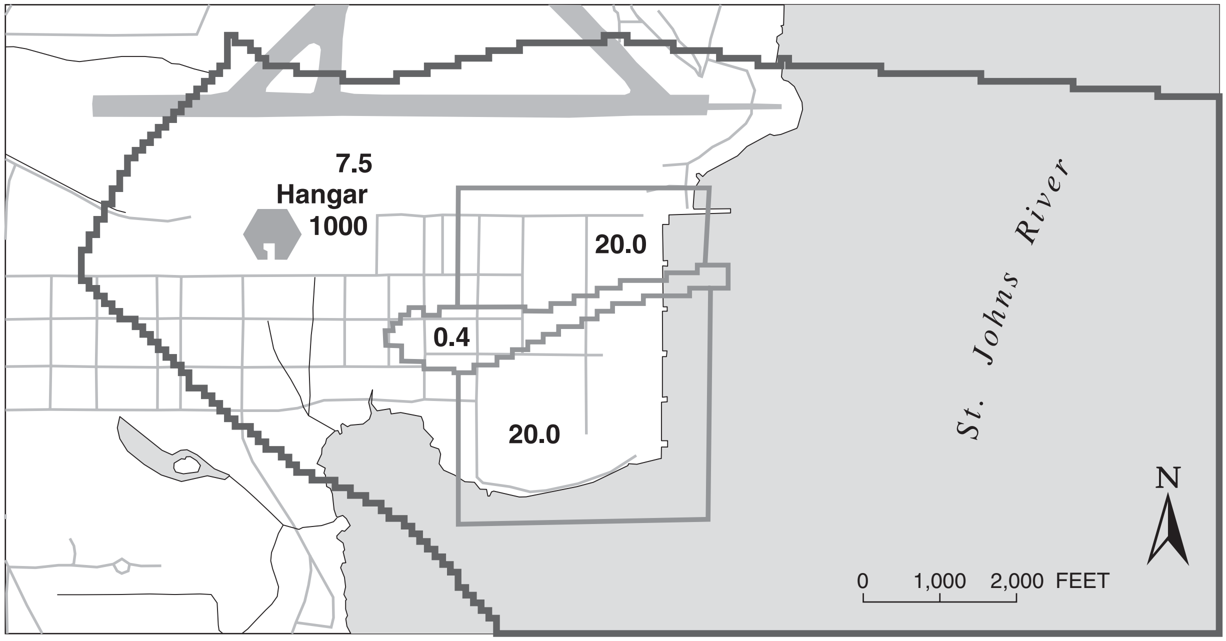

EXPLANATION

SUBREGIONAL STUDY AREA AND SUBREGIONAL MODEL BOUNDARY

BOUNDARY OF MODEL-SIMULATED HORIZONTAL HYDRAULIC CONDUCTIVITY–Of layer 3

20.0 MODEL-SIMULATED HORIZONTAL HYDRAULIC CONDUCTIVITY–Of layer 3, in feet per day

Figure 26. Simulated horizontal hydraulic conductivity of layer 3 of the recalibrated subregional model.

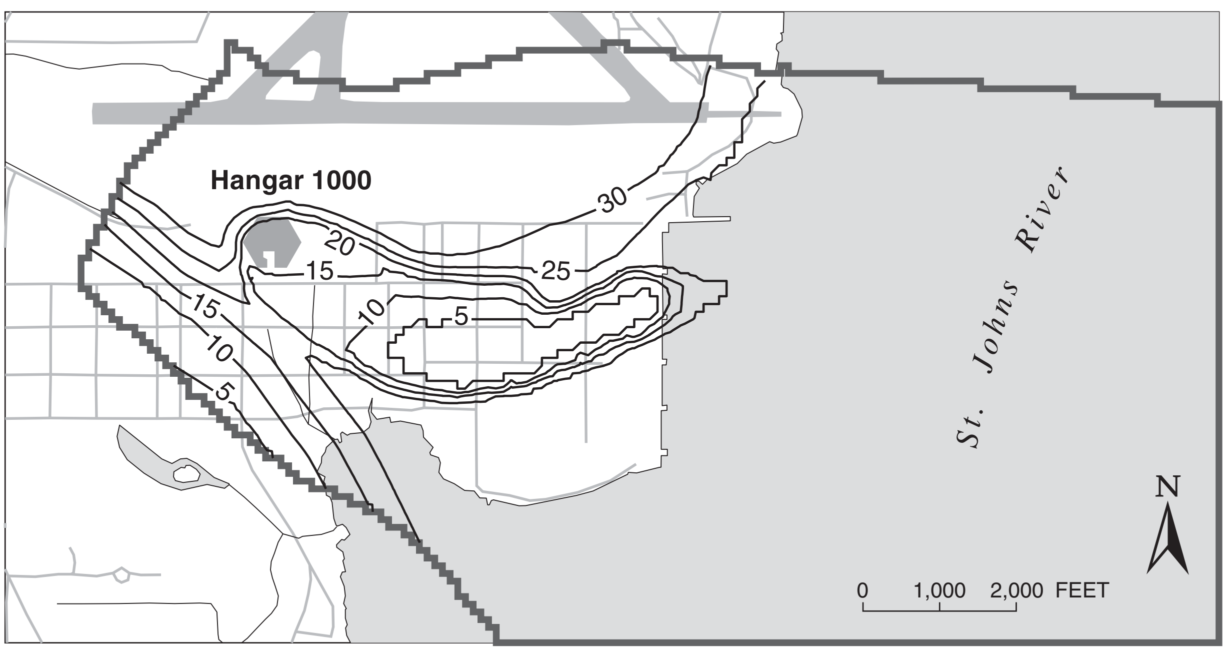

EXPLANATION

SUBREGIONAL STUDY AREA AND SUBREGIONAL MODEL BOUNDARY

5 LINE OF EQUAL SIMULATED THICKNESS OF LAYER 3–Of the subregional model, in feet.

Figure 27. Simulated thickness of layer 3 of the recalibrated subregional model.

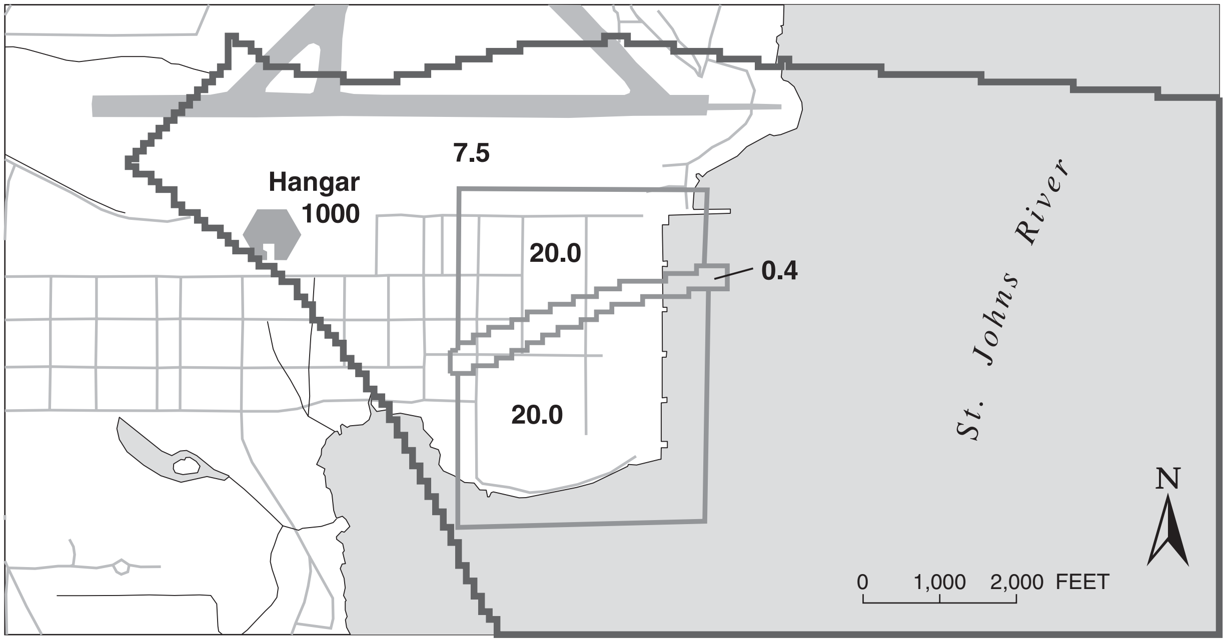

EXPLANATION

SUBREGIONAL STUDY AREA AND SUBREGIONAL MODEL BOUNDARY

BOUNDARY OF MODEL-SIMULATED HORIZONTAL HYDRAULIC CONDUCTIVITY–Of layer 4

20.0 MODEL-SIMULATED HORIZONTAL HYDRAULIC CONDUCTIVITY–Of layer 4, in feet per day

Figure 28. Simulated horizontal hydraulic conductivity of layer 4 of the recalibrated subregional model.

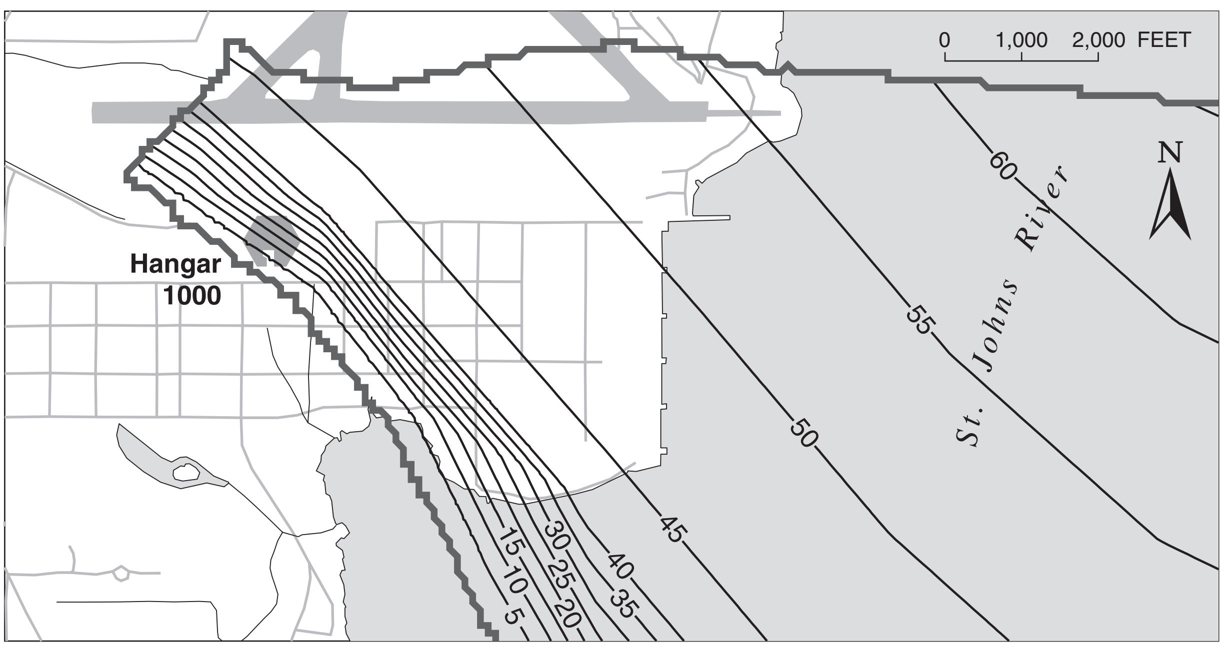

EXPLANATION

SUBREGIONAL STUDY AREA AND SUBREGIONAL MODEL BOUNDARY

—5— LINE OF EQUAL SIMULATED THICKNESS OF LAYER 4–Of the subregional model, in feet.

Figure 29. Simulated thickness of layer 4 of the recalibrated subregional model.

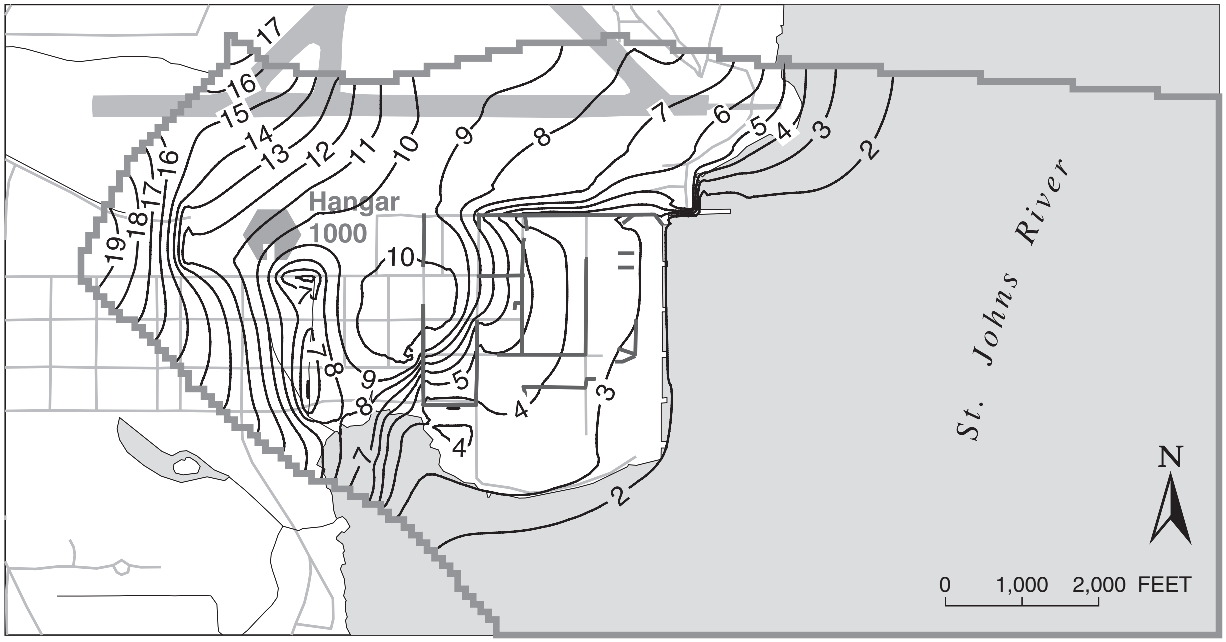

EXPLANATION

SUBREGIONAL STUDY AREA AND SUBREGIONAL MODEL BOUNDARY

5 SIMULATED WATER-TABLE CONTOUR–Shows model-simulated head in the upper layer. Contour interval 1 foot. Datum is NGVD of 1929

SIMULATED LEAKING STORMWATER DRAINS

Figure 30. Simulated water-table surface of the upper layer of the recalibrated subregional model.

The calibrated conductances of the stormwater drains ranged from 0.1 to 2 ft^2/d. All of these values are the same as the values used in the original subregional model except the stormwater drains, which had a lower conductance.

The simulated water table for the upper layer is shown in figure 30. The water table slopes toward the St. Johns River except in areas that are influenced by the leaking stormwater drains. Almost all of the simulated drains caused some depression in the water-table surface because they are removing ground water from the upper layer of the aquifer. The presence of the seawall causes elevated heads to occur directly adjacent to the St. Johns River in the central and northern parts of OU3. The heads are relatively higher in this area because the seawall extends downward into the clay and prevents ground water from moving easily under the seawall and discharging to the St. Johns River.

The simulated potentiometric surface for the intermediate layer slopes toward the St. Johns River (fig. 31). The presence of the low-permeability deposits is reflected in the bending of the contours in the central part of OU3; the result is a steeper slope of the potentiometric surface in the northern half of OU3 than in the southern half.

Ideally, there would also be a match of simulated flows to field measurements. Two streamflow measurements were taken within the study area (fig. 9); however, as discussed earlier, these creeks receive both ground-water seepage and flow from other sources, and thus could only be used as an upper limit for comparison with model-simulated values which were substaintially below the measured values. The regional, Station-wide ground-water model was calibrated to measured stream flows (due to numerous creeks at the Station) and the same recharge rates determined in adjacent watersheds were applied to the recalibrated modeled watershed to ensure reasonable recharge rates.

Ground-Water Budget

The model-simulated inflows and outflows for the subregional model area are shown in table 4. The total rate of recharge to the subregional model was

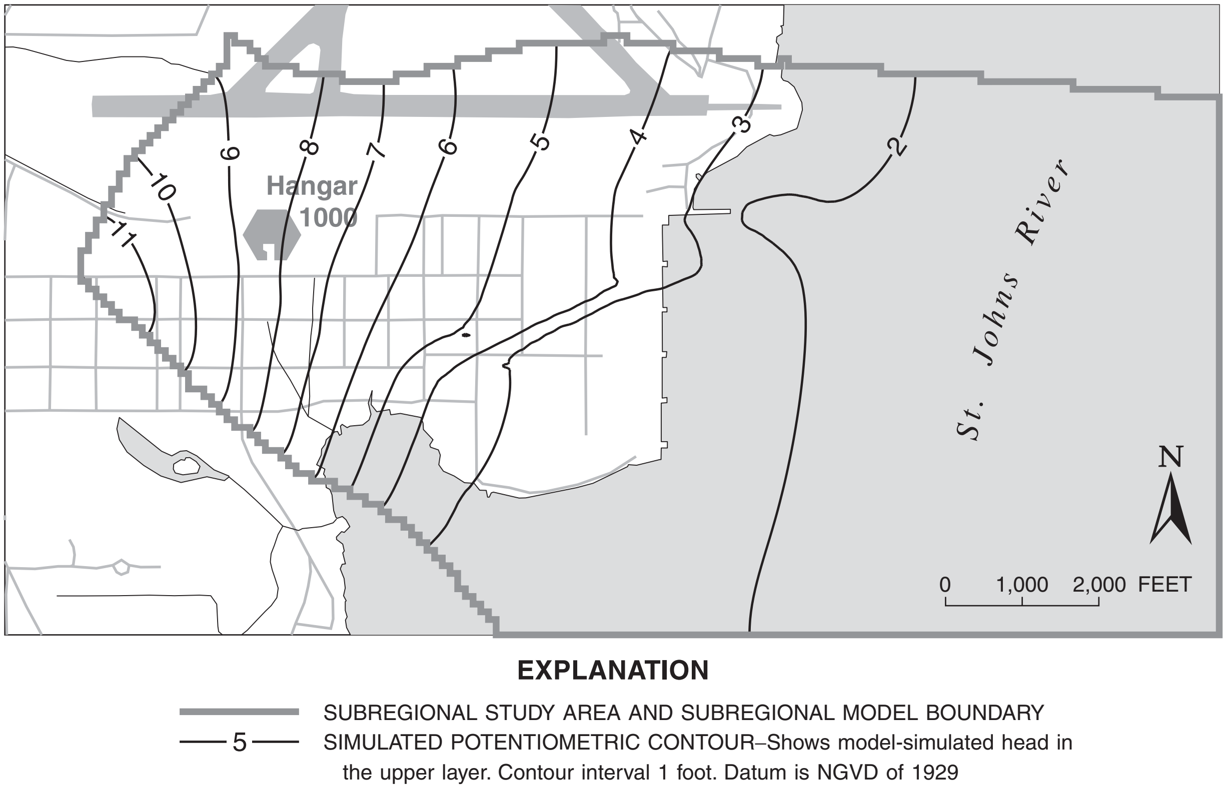

Figure 31. Simulated potentiometric surface of the intermediate layer of the recalibrated subregional model.

0.189 ft^3/s. Discharge rates were 0.071 ft^3/s to the St. Johns River, 0.055 ft^3/s to the ditches, and 0.063 ft^3/s to the stormwater drains.

Table 4. Simulated ground-water inflows and outflows for the recalibrated subregional model

[ft^3/s, cubic feet per second]

Ground-water source or sink	Flow rate into the model (ft^3/s)	Flow rate out of the model (ft^3/s)
Recharge	0.189	0
St. Johns River	0	0.071
Ditches	0	0.055
Stormwater drains	0	0.063
Total	0.189	0.189

Sensitivity Analysis

Sensitivity tests were conducted to determine the effect of changes in model input parameters on the model calibration. Tests were conducted by increasing (or decreasing) each parameter by 50 percent while other parameters were unchanged. Parameter changes resulted in the simulation of a new distribution of heads, and the effect of the parameter change was judged by determining the number of simulated heads that no longer remained within 1.5 ft of the measured values (table 5). Input parameters tested were recharge, riverbed conductance, storm drain conductance, horizontal hydraulic conductivity of the upper layer, horizontal hydraulic conductivity of the clay layer, horizontal hydraulic conductivity of the intermediate layer, and vertical hydraulic conductivity.

The model was sensitive to recharge rate changes because recharge was the only source of water to the model. Decreasing the recharge rate by 50 percent caused the simulated heads to drop and the number of simulated heads exceeding the error criterion to increase from 1 to 6 (out of 46). Increasing the recharge rate by 50 percent caused the model heads to rise and the number of heads exceeding the error criterion to increase from 1 to 10.

Decreasing the riverbed conductance caused the simulated heads to rise, because a larger gradient was necessary to move water from the aquifer to the river. A decrease of 50 percent caused the total number of simulated heads exceeding the error criterion to increase from 1 to 5. In contrast, the model was not sensitive to increases in riverbed conductance. An increase of 50 percent caused the number of simulated heads exceeding the error criterion to increase from 1 to 3.

Decreasing the storm drain conductance caused simulated heads in the vicinity of the drains to rise, because a larger vertical gradient developed between the drains and the aquifer. A decrease of 50 percent caused the number of simulated heads exceeding the error criterion to increase from 1 to 5 in the upper layer. The model was not sensitive to an increase in drain conductance. An increase of 50 percent caused the number of simulated heads exceeding the error criterion in the upper layer to increase from 1 to 3. As expected, varying the drain conductance had little effect on the heads in the intermediate layer.

Decreasing the horizontal hydraulic conductivity in the upper layer by 50 percent caused no change in the number of heads that exceeded the error criterion. This is probably because most of the wells are near storm drains, which reduce the fluctuations of the water levels in the aquifer in their vicinity. An increase of 50 percent also caused no change in the quality of the calibration for the same reason.

Increasing or decreasing the horizontal hydraulic conductivity in the clay layer by 50 percent also caused no change in the number of heads that exceeded the error criterion. This is probably because the clay layer had a low conductivity (especially in the thicker areas) and varying this low conductivity did not substantially change the volume of water moving through it.

Decreasing the horizontal hydraulic conductivity in the intermediate layer (layers 3 and 4 combined) caused the simulated heads in the intermediate layer to rise, causing a corresponding rise in the upper layer. A decrease of 50 percent caused the total number of simulated heads that exceeded the error criterion to increase from 1 to 6. The model was not sensitive to an increase in horizontal hydraulic conductivity. An increase of 50 percent caused no change in the quality of the calibration.

Decreasing the vertical hydraulic conductivity by 50 percent caused simulated heads in layer 1 to rise and the total number of simulated heads that exceeded the error criterion to increase from 1 to 9. An increase of 50 percent caused no change in the quality of the calibration.

Table 5. Summary of sensitivity analyses for the recalibrated subregional model

[*, indicates parameter is multiplied by the number to the right.]

Parameter changed	Number of simulated heads in the upper layer that exceeded the calibration criterion of 1.5 foot	Number of simulated heads in the intermediate layer that exceeded the calibration criterion of 1.5 foot	Total
Calibrated Model	1	0	1
Recharge * 0.5	4	2	6
Recharge * 1.5	8	2	10
Riverbed conductance * 0.5	4	1	5
Riverbed conductance * 1.5	1	2	3
Drain conductance * 0.5	5	0	5
Drain conductance * 1.5	3	0	3
Horizontal hydraulic conductivity of upper layer * 0.5	1	0	1
Horizontal hydraulic conductivity of upper layer * 1.5	1	0	1
Horizontal hydraulic conductivity of clay layer * 1.5	1	0	1
Horizontal hydraulic conductivity of clay layer * 1.5	1	0	1
Horizontal hydraulic conductivity of intermediate layer * 0.5	6	0	6
Horizontal hydraulic conductivity of intermediate layer * 1.5	1	0	1
Vertical hydraulic conductivity of all layers * 0.5	8	1	9
Vertical hydraulic conductivity of all layers * 1.5	1	0	1

Ground-Water Flow Model Limitations

The subregional model simulated ground-water flow by assuming steady-state conditions. The surficial aquifer is assumed to be under steady-state conditions because water levels in wells showed no long-term trend (but did show seasonal variation). The water table is generally close to the land surface, and there is little capacity for a substantial rise in water levels. If higher than average rainfall occurred, greater runoff would probably result without inducing a substantially higher water table. However, an extended drought could reduce water levels to below those that were used to calibrate the model, which would result in simulated ground-water flow velocities that are slower than actual velocities.

Since there were no discharge measurements for direct calibration of the model, model-derived recharge rates from the Station-wide model (which did have discharge measurements) were used because they were considered to be the best estimates. If these rates were too low, then this would result in ground-water flow velocities that were too low. Conversely, if these recharge rates were too high, then the velocities would be too high.

FATE AND TRANSPORT SIMULATIONS OF TRICHLOROETHENE, DICHLORO-ETHENE, AND VINYL CHLORIDE MOVEMENT AT HANGAR 1000

This section describes site-specific ground-water flow and fate and transport modeling conducted at Hangar 1000. The previously discussed subregional flow model was used to establish layering and boundary conditions for the site-specific ground-water flow model. Fate and transport modeling was conducted using the site-specific ground-water flow model and the computer code, Reactive Transport in Three Dimensions (RT3D), developed by Clement (1997). This code was used because it can simulate the degradation of TCE to DCE to VC. This model is herein referred to as the Hangar 1000 model.

Model Construction

The Hangar 1000 model contains 161 rows and 149 columns of model cells. All cells are 5 ft long on each side. The location and orientation of the finite-difference grid for the Hanger 1000 model is shown in figure 32. The model simulates the same four layers as the subregional model (fig. 20.) The perimeter of the Hangar 1000 model consists of constant head cells; the assigned head at these cells was taken from the calibrated subregional model described in the previous section. All other modeling and aquifer parameters were the same as those used for the subregional model, except for the cell size.

Flow Path Analysis

The direction and rate of ground-water movement in the upper layer of the aquifer was computed by using the USGS program MODPATH (Pollock, 1989), and the results of this analysis are shown in figure 33. Particle tracking was simulated in layer 1 because this is where contaminants are present. The very low-permeability clay layer (layer 2 of the model) essentially prevents contaminate ground water from moving downward into the intermediate layer (layers 3 and 4 of the model) in the study area. Thus, contamination is transported only in layer 1 of the model. The ground-water flow velocity averaged about 75 feet per year (ft/yr) and took about 6 years for particles to move the 450 ft to the storm drain, assuming a porosity of 25 percent. Other porosities would give exactly the same direction of ground-water flow, but the rate of movement would be inversely proportional to the porosity. Reducing the simulated porosity by one half would double the simulated velocity. Likewise, doubling the simulated porosity would decrease the simulated velocity by one half.

Fate and Transport Modeling Overview

The objective of the fate and transport modeling calibration was to match, as closely as possible, the known distribution of TCE, DCE, and VC. Because of the high levels of contamination at the tank removal site, free product is suspected to be present. To simulate this free product source, two cells (creating a 5 by 10 ft area) were designated as constant chemical concentration cells; the concentration in these two cells was varied during calibration. When a simulation began, RT3D assigned particles to constant concentration model cells; each particle represented a cell volume-weighted mass of contamination. The movement of particles was tracked during each step in the simulation.

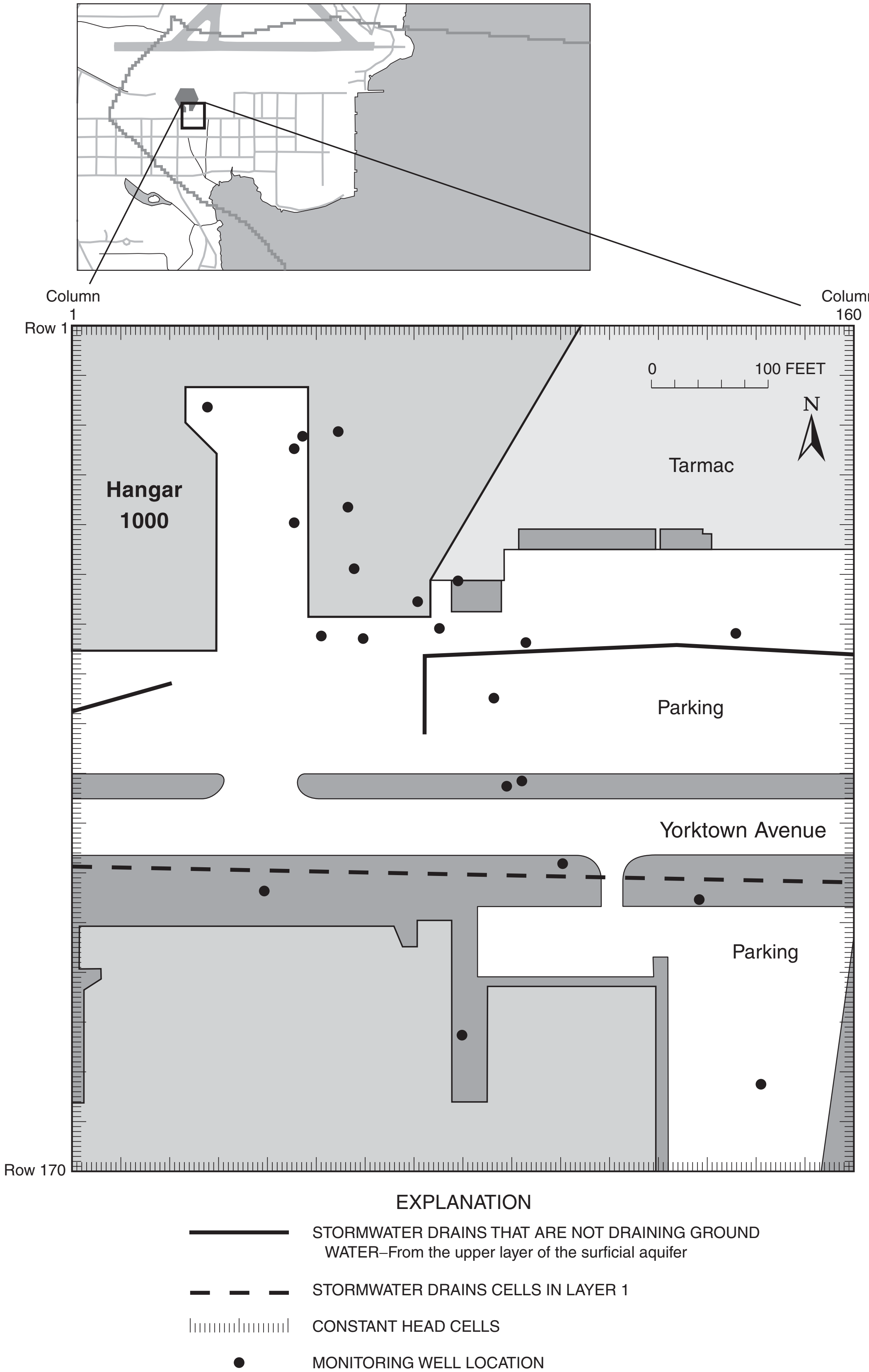

Figure 32. Location and orientation of the Hangar 1000 model.

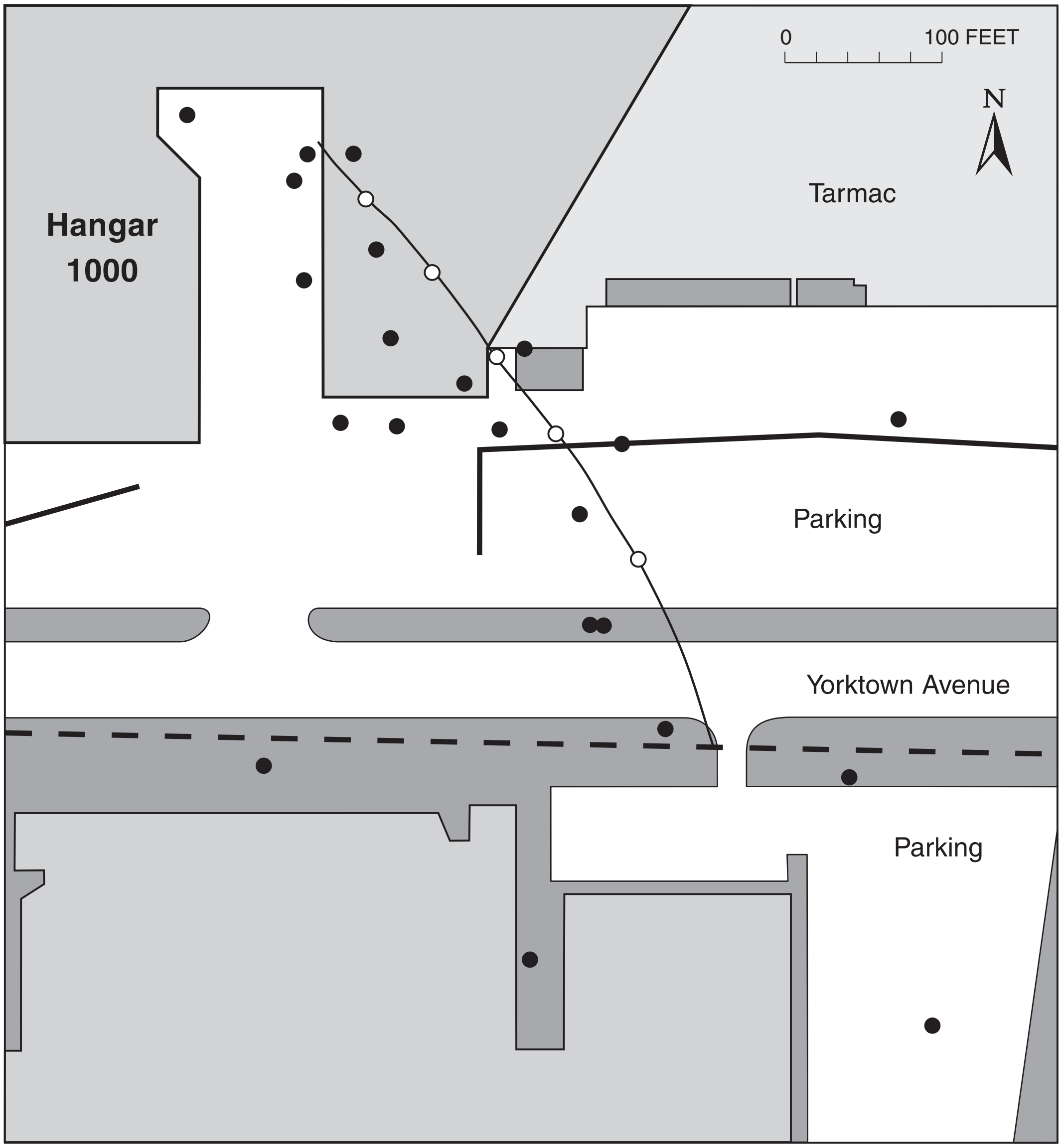

EXPLANATION

STORMWATER DRAINS THAT ARE NOT DRAINING GROUND WATER–From the upper layer of the surficial aquifer

STORMWATER DRAINS THAT ARE DRAINING GROUND WATER–From the upper layer of the surficial aquifer

PARTICLE PATHLINE–Shows simulated ground-water flow path in the upper layer. Distance between dots represents a traveltime of 1 year

MONITORING WELL LOCATION

Figure 33. Particle pathlines representing ground-water flow directions in the upper layer of the surficial aquifer at Hangar 1000.

The sum of the masses of all the particles in a cell equaled the total mass of contamination for that cell. Advection of ground water is the most important factor governing the transport of these chemical compounds. The direction of ground-water flow was determined from the intercell flow velocities, which were part of the output from MODFLOW. The intercell flow velocities were divided by the effective porosity to get the ground-water velocity. In addition to advection, the effects of retardation, hydrodynamic dispersion, and chemical decay were added to the simulation. The effects of retardation due to sorption caused the contaminant to move slower than the ground water, and these effects were specified by the retardation factor. The effect of hydrodynamic dispersion, as specified by the dispersivity, caused the plume to spread. Chemical decay, as specified by a half-life, dictated how rapidly the compounds degraded naturally in the aquifer. TCE degrades into DCE; DCE degrades into VC; and VC can degrades into ethene (or VC could be biodegraded to other non-hazardous compounds). For a more complete discussion of contaminant transport, see Zheng and Bennett (1995).

The calibration strategy was to vary the effective porosity, dispersivity, retardation, chemical decay rate, and chemical concentrations in two constant chemical concentration cells (that represented the source area) until modeled concentrations matched measured values as closely as possible. For this simulation, it was assumed that the flow field is constant in time, degradation and sorption are constant along a flow path, and that degradation occurs in both the dissolved and sorbed phase.

After the fate and transport model was calibrated, it was used to simulate future concentrations. The Navy has begun pilot tests to reduce the concentrations at the tank removal site. To simulate this result the concentration in the constant concentration cells was reduced by 50 percent and the model was run to predict the effect. This scenerio was then repeated assuming a 100 percent reduction at the source.

Calibration to Current Distributions of Trichloroethene, Dichloroethene, and Vinyl Chloride

As discussed earlier, the simulated source of contamination is the two constant chemical concentration cells (creating a source area of 5 by 10 ft) located where the leaking chemical storage tank and associated piping existed before removal. The calibrated values for the two constant chemical concentration cells were 11,000 and 20,000 μg/L for TCE; 5,400 and 10,000 μg/L for DCE; and 0 and 0 μg/L for VC. Figure 34 shows the simulated TCE distribution 16 years after the initial release. The spilled product acts as an ongoing source by slowly leaching into the ground water. TCE then continues moving toward, and discharging into, the stormwater sewer to the southeast. It is not known when the release of TCE actually began, but the tanks were installed in the late 1960s, approximately 35 years ago. After simulating 16 years into the future, TCE concetrations reach steady-state conditions; that is, the concentrations do not change if additional years are simulated. Since these steady-state concentrations result in the best match to the measured data, it is speculated that the initial leak occurred more than 16 years ago. If the contamination source area changed sunstantially during tank removal in 1994, then some concentration changes may still be migrating through the system. DCE concentrations reached steady-state conditions in 14 years (fig. 35) and VC concentrations reached steady-state concentrations in 12 years (fig 36). The VC concentrations reached steady-state conditions first because the retardation factor for VC is the lowest of the three chemicals, thus allowing VC to be transported faster; DCE was intermediate in reaching steady-state conditions because its retardation factor is intermediate to TCE and VC.

At monitoring well H10-MW08 (map number 12) located directly south of the simulated source area, the model-simulated and measured TCE concentrations are 8,609 and 8,710 μg/L (fig. 34), respectively; the model-simulated and measured DCE concentrations are 3,779 and 4,280 μg/L (fig. 35), respectively. Matching the concentrations at this well was used as the basis for determining the concentration level in the two constant chemical concentration cells. The concentration for VC was set at 0 μg/L in the source area because VC is a degradation product of DCE. Matching the measured concentration values in the other wells was accomplished by varying the dispersivity and first order decay rates of TCE, DCE, and VC. The dispersivity values that gave the best match were: longitudinal 1.5 ft, transverse 0.27 ft, and vertical 0.27 ft. These dispersivity values fall within the expected range (0.98 to 5.6 ft for longitudinal and 0.033 to 0.3 ft for transverse dispersivity) described by Gelhar and others (1992).

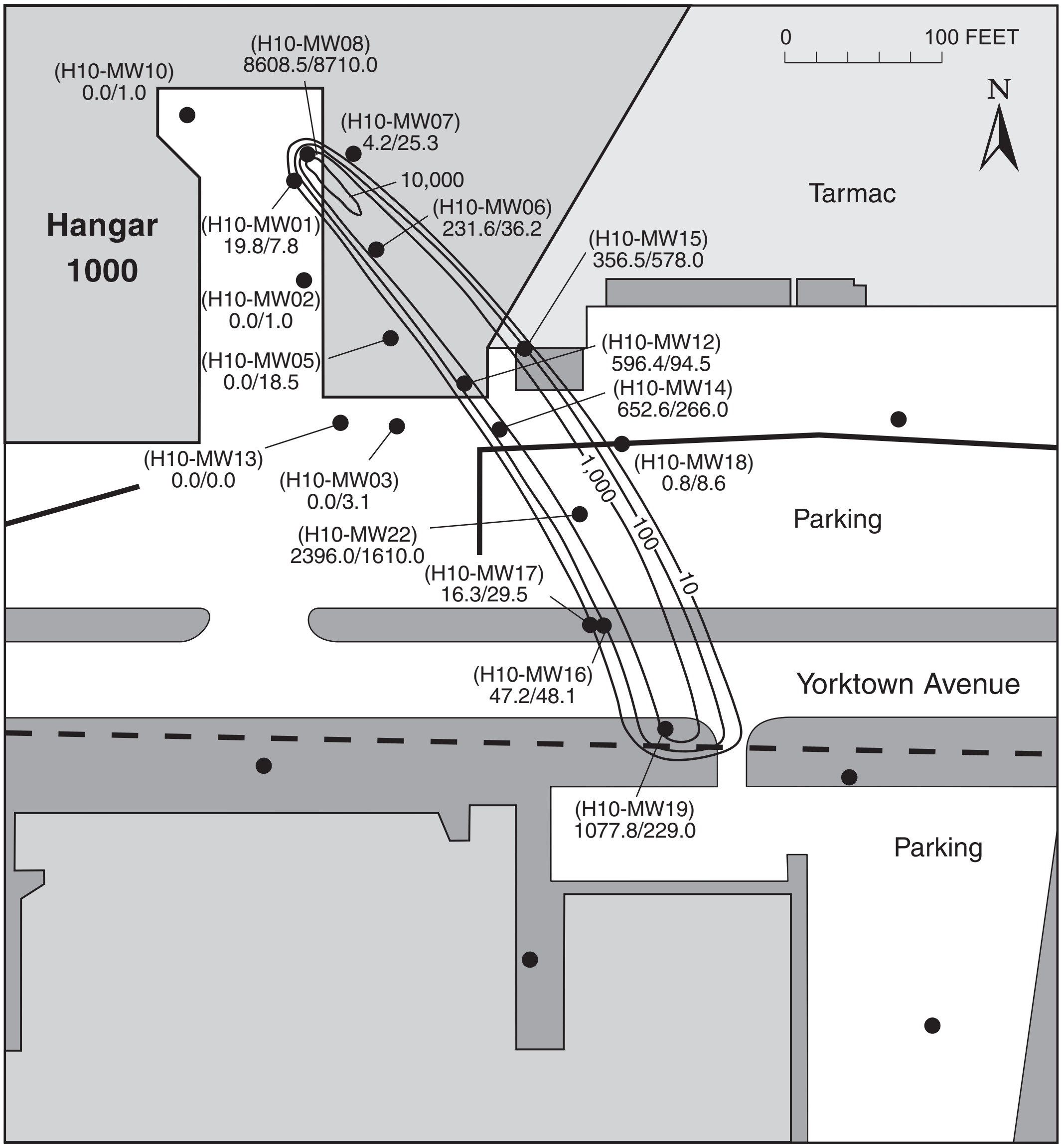

EXPLANATION

STORMWATER DRAINS THAT ARE NOT DRAINING GROUND WATER–From the upper layer of the surficial aquifer

STORMWATER DRAINS THAT ARE DRAINING GROUND WATER–From the upper layer of the surficial aquifer

—10— LINE OF EQUAL SIMULATED TCE CONCENTRATION–In micrograms per liter. Interval is variable

● MONITORING WELL LOCATION
(H10-MW16) (WELL NAME)
47.2/48.1 SIMULATED/OBSERVED CONCENTRATION–In micrograms per liter

Figure 34. Simulated trichloroethene (TCE) concentrations in layer 1 after 16 years.

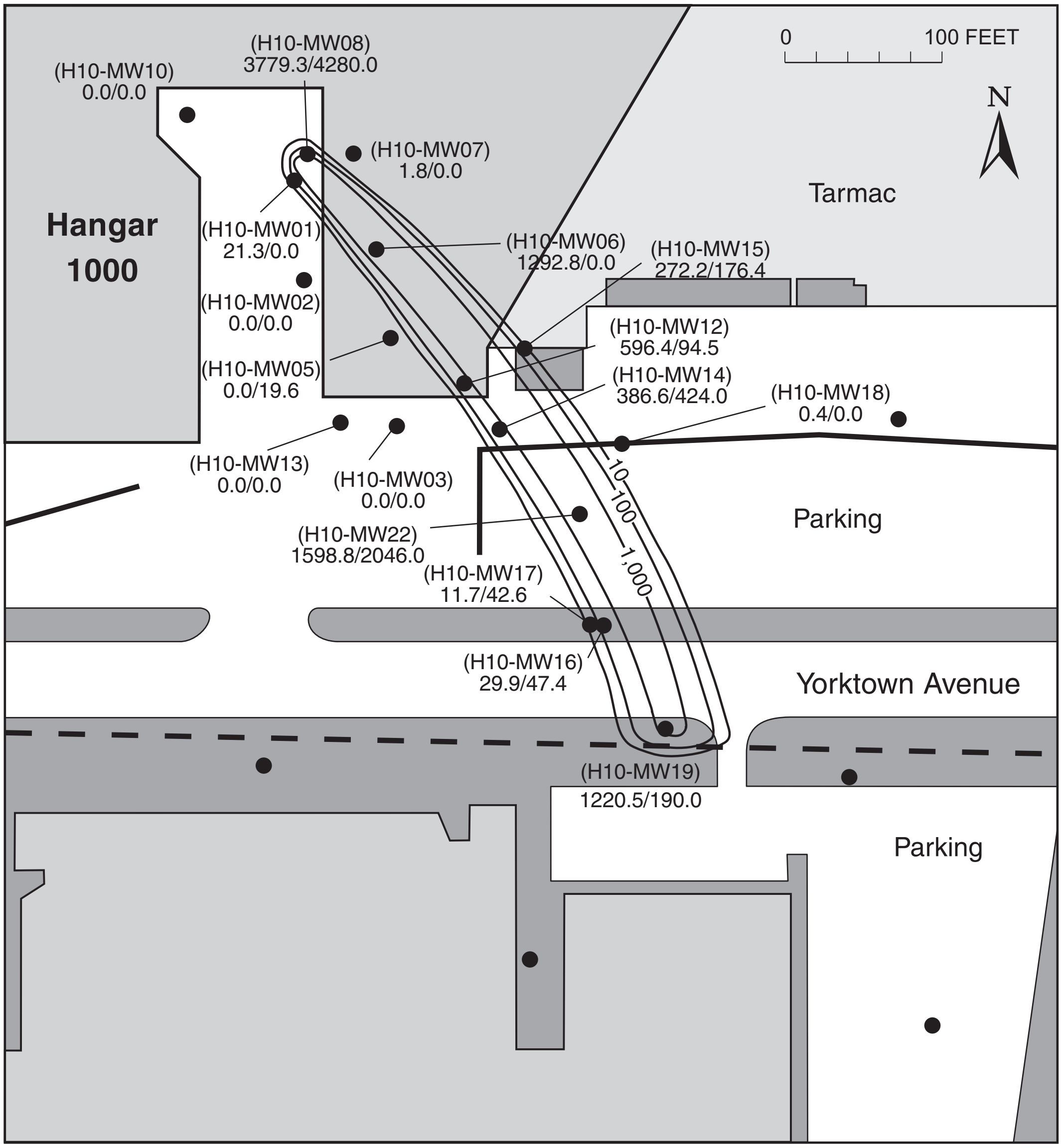

EXPLANATION

——	STORMWATER DRAINS THAT ARE NOT DRAINING GROUND WATER–From the upper layer of the surficial aquifer
– – –	STORMWATER DRAINS THAT ARE DRAINING GROUND WATER–From the upper layer of the surficial aquifer
——10——	LINE OF EQUAL SIMULATED DCE CONCENTRATION–In micrograms per liter. Interval is variable
●	MONITORING WELL LOCATION
(H10-MW19)	(WELL NAME)
1220.5/190.0	SIMULATED/OBSERVED CONCENTRATION–In micrograms per liter

Figure 35. Simulated dichloroethene (DCE) concentrations in layer 1 after 14 years.

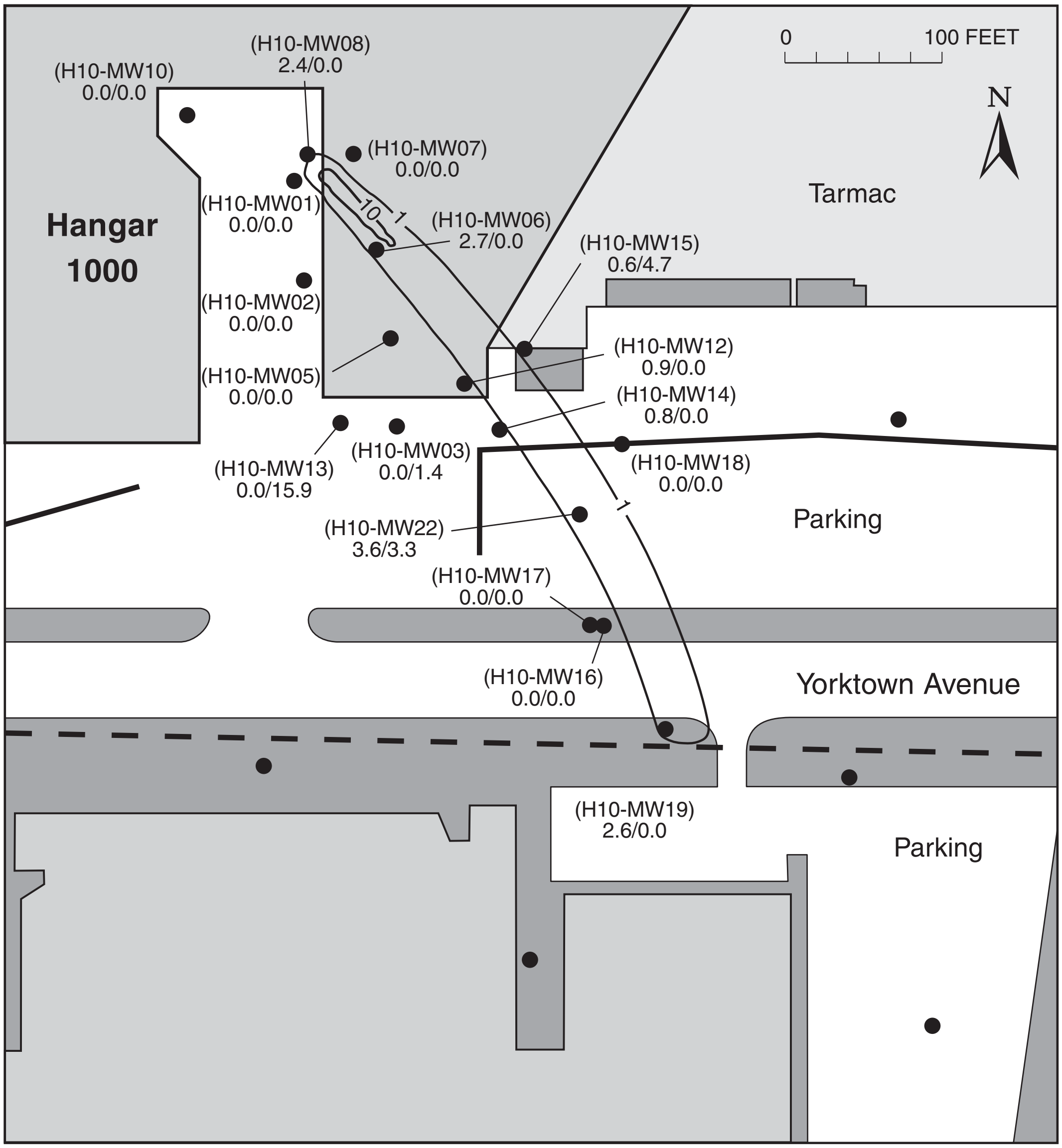

EXPLANATION

STORMWATER DRAINS THAT ARE NOT DRAINING GROUND WATER–From the upper layer of the surficial aquifer

STORMWATER DRAINS THAT ARE DRAINING GROUND WATER–From the upper layer of the surficial aquifer

——10—— LINE OF EQUAL SIMULATED VC CONCENTRATION–In micrograms per liter. Interval is variable

● MONITORING WELL LOCATION
(H10-MW19) (WELL NAME)
2.6/0.0 SIMULATED/OBSERVED CONCENTRATION–In micrograms per liter

Figure 36. Simulated vinyl chloride (VC) concentrations in layer 1 after 12 years.

Because the discharge point was close to the source (about 450 ft), the model was relatively insensitive to dispersivity. Dispersivity has the greatest effect on contaminant concentrations when the contamination has a long distance to travel and thus has a long period to affect the plume.

The first order decay rate for TCE that resulted in the best match was 0.0002 d^{-1}. At a similar site at OU3 (the contamination was near the water table and the site was paved), 10 years of measuring TCE concentrations gave first order decay rates of 0.0007 to 0.0002 d^{-1} (U.S. Navy, 1998). The expected range of values for TCE is 0.0002 to 0.08 d^{-1} (U.S. Environmental Protection Agency, 1998). At this site, the simulated degradation rate of TCE that gave the best match was at the slow end of the expected range. The calibrated first order decay rate was a 0.0002 for DCE and 0.06 d^{-1} for VC. The expected range of values for VC is 0.0006 to 0.08 d^{-1} (U.S. Environmental Protection Agency, 1998). A relatively high decay rate (but still within the expected range) for VC was required to match the low concentration values observed at the site. At Cecil Field, located about 10 miles west of the Jacksonville Naval Air Station, a low TCE decay rate and a high VC decay rate also were observed and attributed to the mildly oxidizing conditions (Frank Chapelle, U.S. Geological Survey written commun., 2002).

Figure 37 shows the simulated TCE distribution 8 years after the initial release of contamination. As shown in figure 37, the TCE plume has moved only about one-half of the distance to the storm sewer.

Predicted Movement of Trichloroethene, Dichloroethene, and Vinyl Chloride Assuming Source Reduction of 50 Percent

The effect of the reduction in the concentration of contamination at the source was simulated. For these simulations, the source was reduced by 50 percent. Figure 38 shows the simulated distribution of TCE 8 years after the source reduction. The 3,000-µg/L concentration contour near the center of the plume represents the last of the higher concentrations of TCE contamination that left the source and have traveled about one-half of the distance to the storm sewer. For all of the contaminants, the new steady-state concentrations were one-half of the original concentrations.

Figures 39 and 40 show the simulated distribution of DCE and VC, respectively, 8 years after the source reduction. The 2,000-µg/L concentration contour (fig. 39) near the center of the plume represents the last of the higher concentrations of DCE contamination that left the source and have traveled about one-half of the distance to the storm sewer.

Predicted Movement of Trichloroethene, Dichloroethene, and Vinyl Chloride Assuming Source Reduction of 100 Percent

In these simulations, the reduction in the concentration of contamination at the source was 100 percent. Figures 41- 43 show the simulated distributions of TCE, DCE, and VC, respectively, 8 years after the source was eliminated. As shown in these figures, TCE, DCE, and VC are absent from ground water in the area where the tanks were located, and the remainder of the contaminant plumes have moved toward the storm sewer.

Figure 44 shows the simulated distribution of TCE 16 years after source elimination. The TCE-contaminated ground water has been flushed almost completely from the aquifer. Since TCE was not completely removed from the aquifer after 16 years, it apparently takes slightly longer for the contaminant to be flushed from the aquifer than it did for the initial concentrations to reach the storm sewer after the initial release. The simulated period of time for the contaminants to be removed from the aquifer once the source was removed was about 17 years for TCE, 15 years for DCE, and 13 years for VC.

Measurement Error and Effect of Parameter Variation on Fate and Transport Modeling Results

The simulation of future contaminant concentration values and the times of arrival at the storm sewer are subject to three major sources of error. First, the simulated ground-water flow velocities may not accurately reflect the actual flow velocities; second, the measured concentrations may not fully characterize the contaminant concentrations in the aquifer; and third, the model input parameters may not accurately characterize the transport mechanisms.

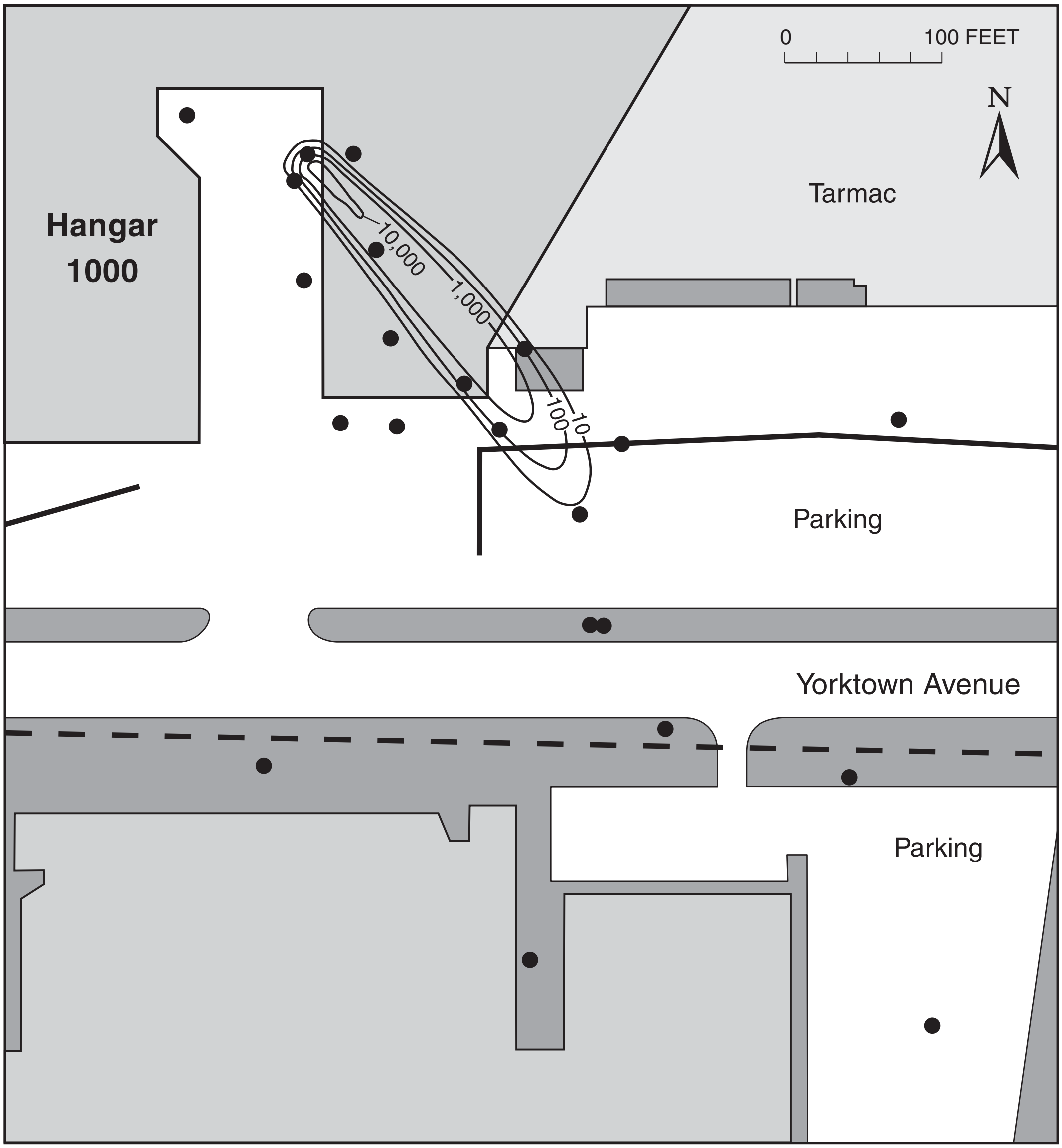

EXPLANATION

STORMWATER DRAINS THAT ARE NOT DRAINING GROUND WATER–From the upper layer of the surficial aquifer

STORMWATER DRAINS THAT ARE DRAINING GROUND WATER–From the upper layer of the surficial aquifer

10 LINE OF EQUAL SIMULATED TCE CONCENTRATION–In micrograms per liter. Interval is variable

MONITORING WELL LOCATION

Figure 37. Simulated trichloroethene (TCE) concentrations in layer 1 after 8 years.

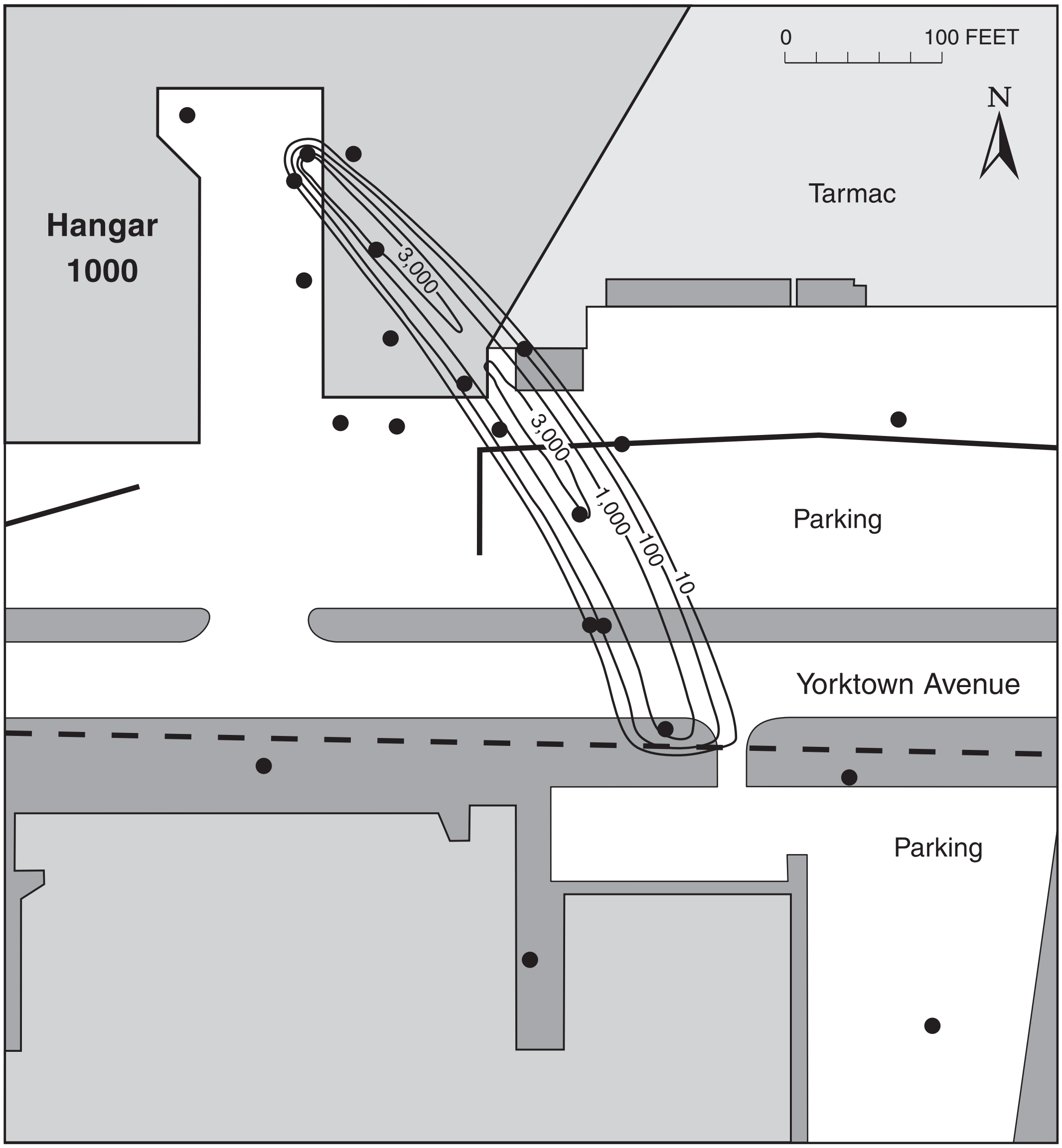

EXPLANATION

STORMWATER DRAINS THAT ARE NOT DRAINING GROUND WATER–From the upper layer of the surficial aquifer

STORMWATER DRAINS THAT ARE DRAINING GROUND WATER–From the upper layer of the surficial aquifer

—10— LINE OF EQUAL SIMULATED TCE CONCENTRATION–In micrograms per liter. Interval is variable

● MONITORING WELL LOCATION

Figure 38. Simulated trichloroethene (TCE) concentrations in layer 1 after 8 years assuming 50 percent source reduction.

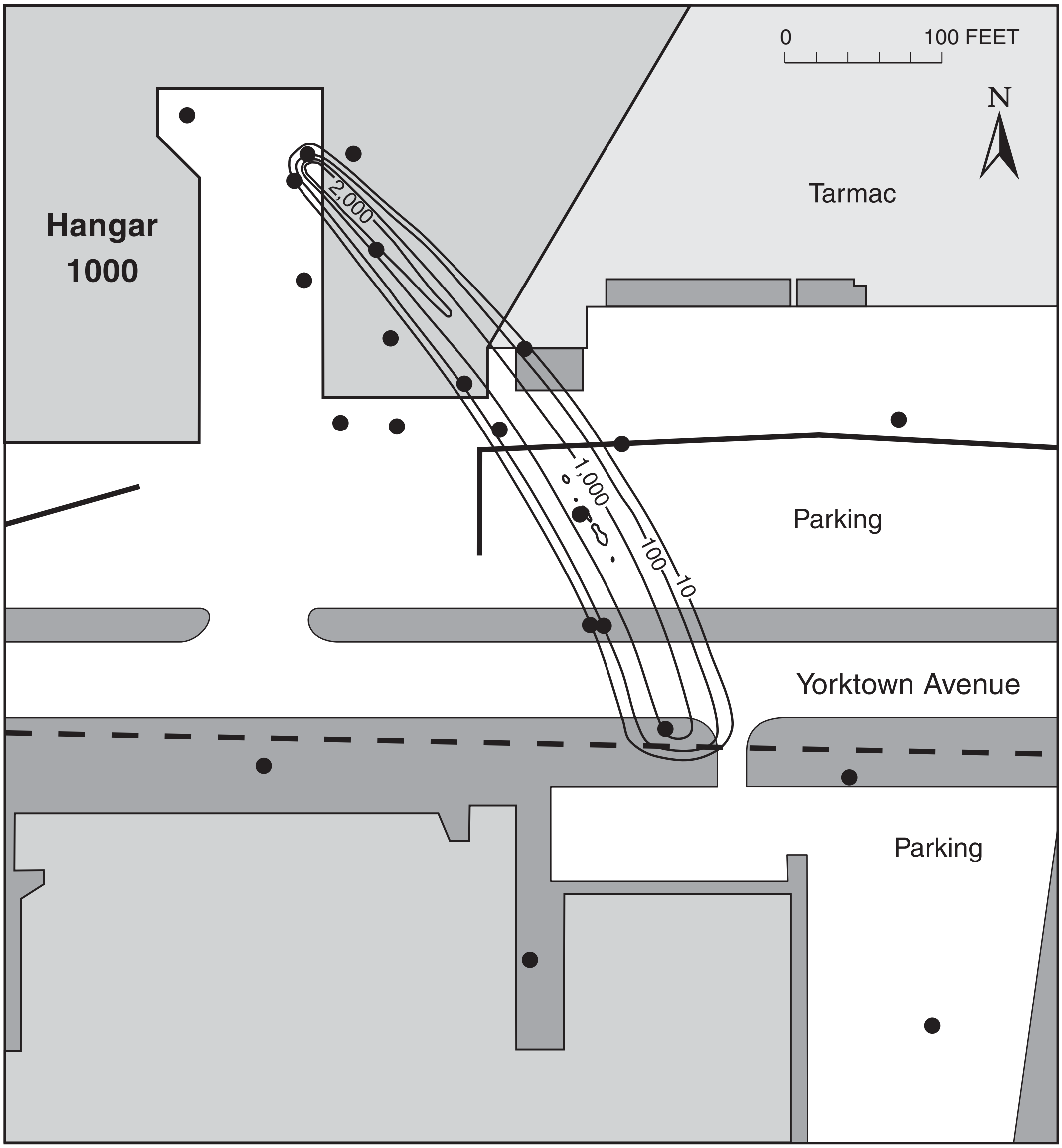

EXPLANATION

STORMWATER DRAINS THAT ARE NOT DRAINING GROUND WATER–From the upper layer of the surficial aquifer

STORMWATER DRAINS THAT ARE DRAINING GROUND WATER–From the upper layer of the surficial aquifer

10 LINE OF EQUAL SIMULATED DCE CONCENTRATION–In micrograms per liter. Interval is variable

MONITORING WELL LOCATION

Figure 39. Simulated dichloroethene (DCE) concentrations in layer 1 after 8 years assuming 50 percent source reduction.

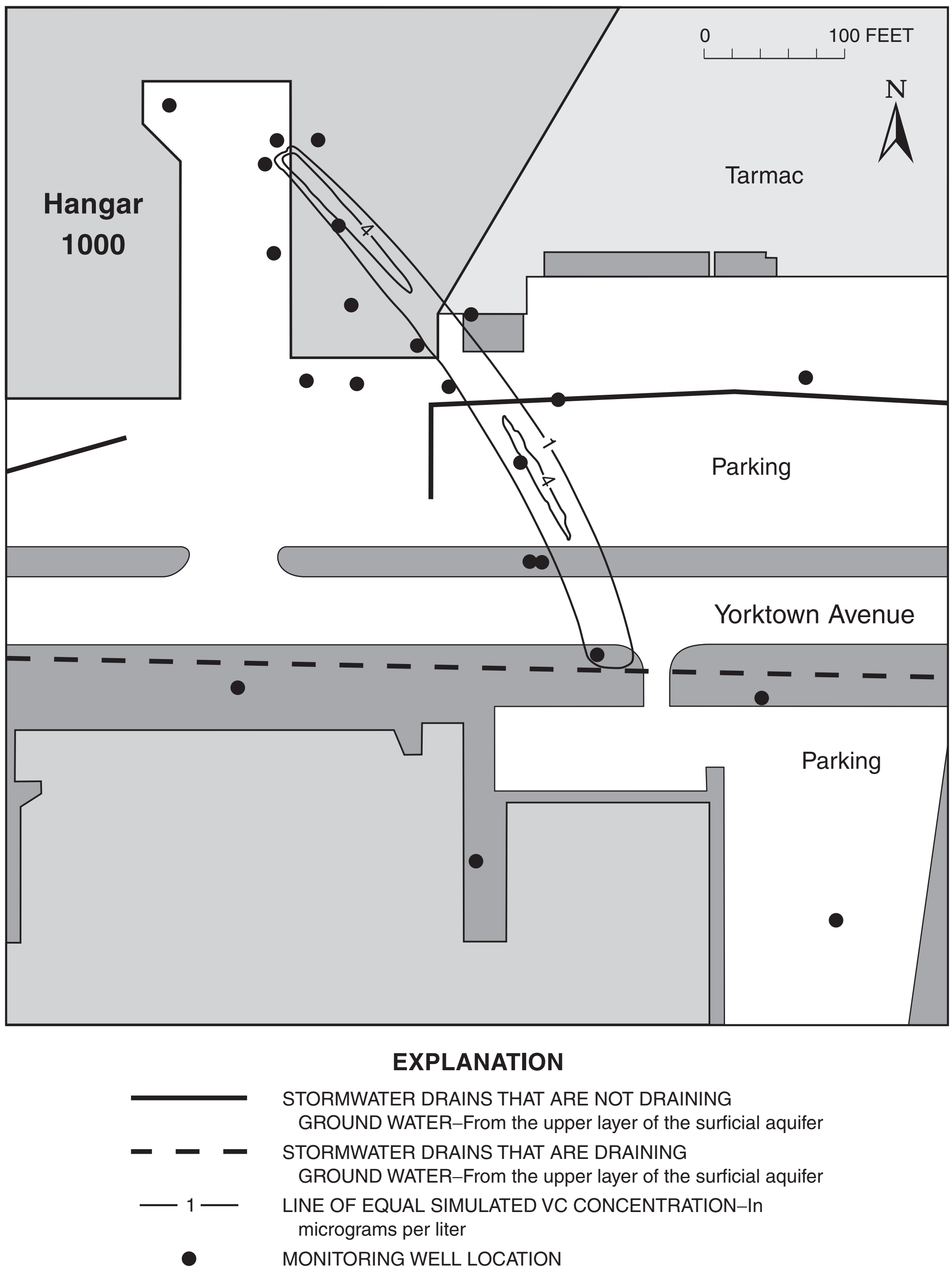

Figure 40. Simulated vinyl chloride (VC) concentrations in layer 1 after 8 years assuming 50 percent source reduction.

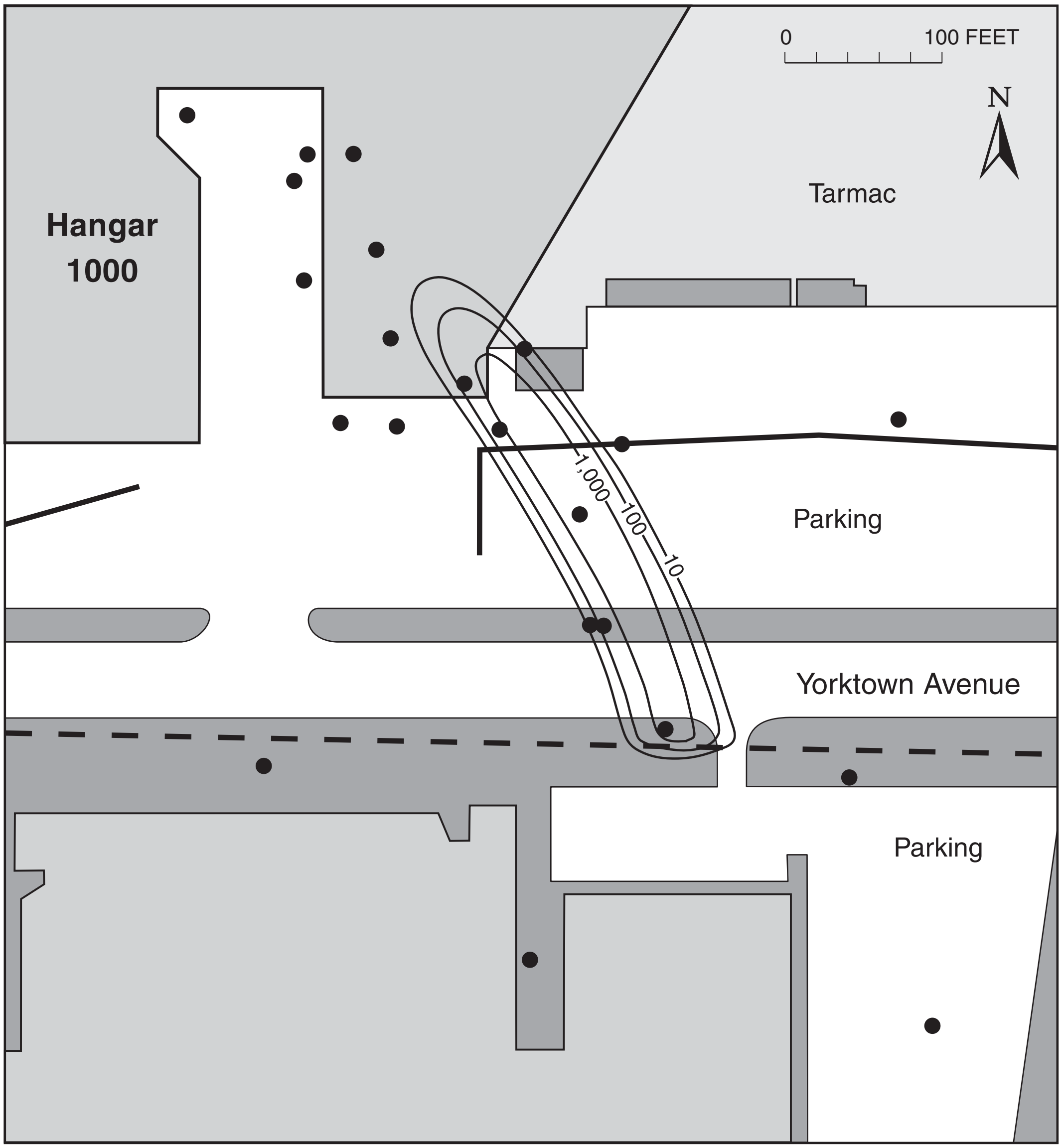

EXPLANATION

- STORMWATER DRAINS THAT ARE NOT DRAINING GROUND WATER–From the upper layer of the surficial aquifer
- STORMWATER DRAINS THAT ARE DRAINING GROUND WATER–From the upper layer of the surficial aquifer
- —10— LINE OF EQUAL SIMULATED TCE CONCENTRATION–In micrograms per liter. Interval is variable
- ● MONITORING WELL LOCATION

Figure 41. Simulated trichloroethene (TCE) concentrations in layer 1 after 8 years assuming 100 percent source reduction.

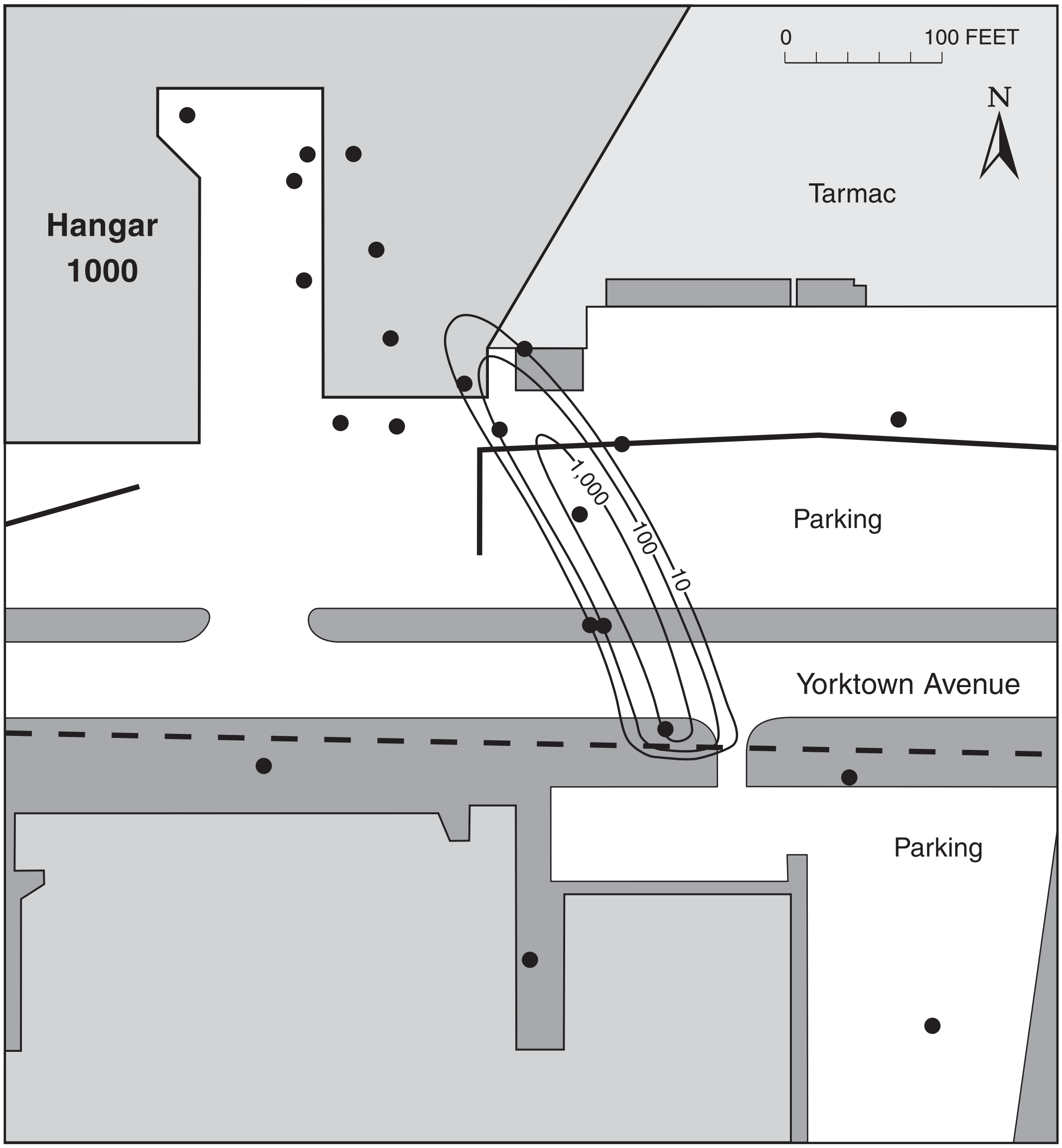

EXPLANATION

STORMWATER DRAINS THAT ARE NOT DRAINING GROUND WATER–From the upper layer of the surficial aquifer

STORMWATER DRAINS THAT ARE DRAINING GROUND WATER–From the upper layer of the surficial aquifer

10 LINE OF EQUAL SIMULATED DCE CONCENTRATION–In micrograms per liter. Interval is variable

MONITORING WELL LOCATION

Figure 42. Simulated dichloroethene (DCE) concentrations in layer 1 after 8 years assuming 100 percent source reduction.

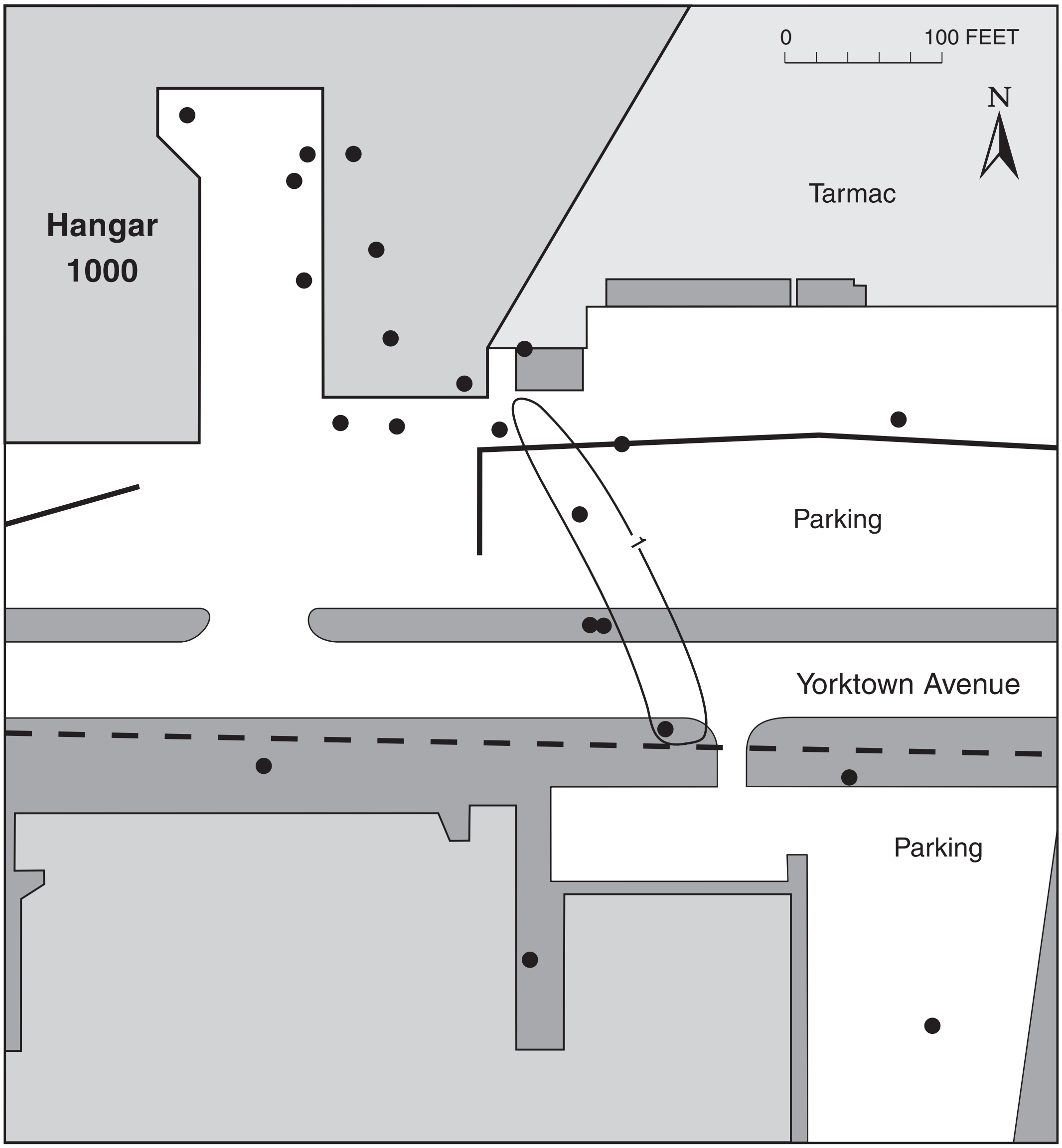

EXPLANATION

STORMWATER DRAINS THAT ARE NOT DRAINING GROUND WATER–From the upper layer of the surficial aquifer

STORMWATER DRAINS THAT ARE DRAINING GROUND WATER–From the upper layer of the surficial aquifer

1 LINE OF EQUAL SIMULATED VC CONCENTRATION–In micrograms per liter

MONITORING WELL LOCATION

Figure 43. Simulated vinyl chloride (VC) concentrations in layer 1 after 8 years assuming 100 percent source reduction.

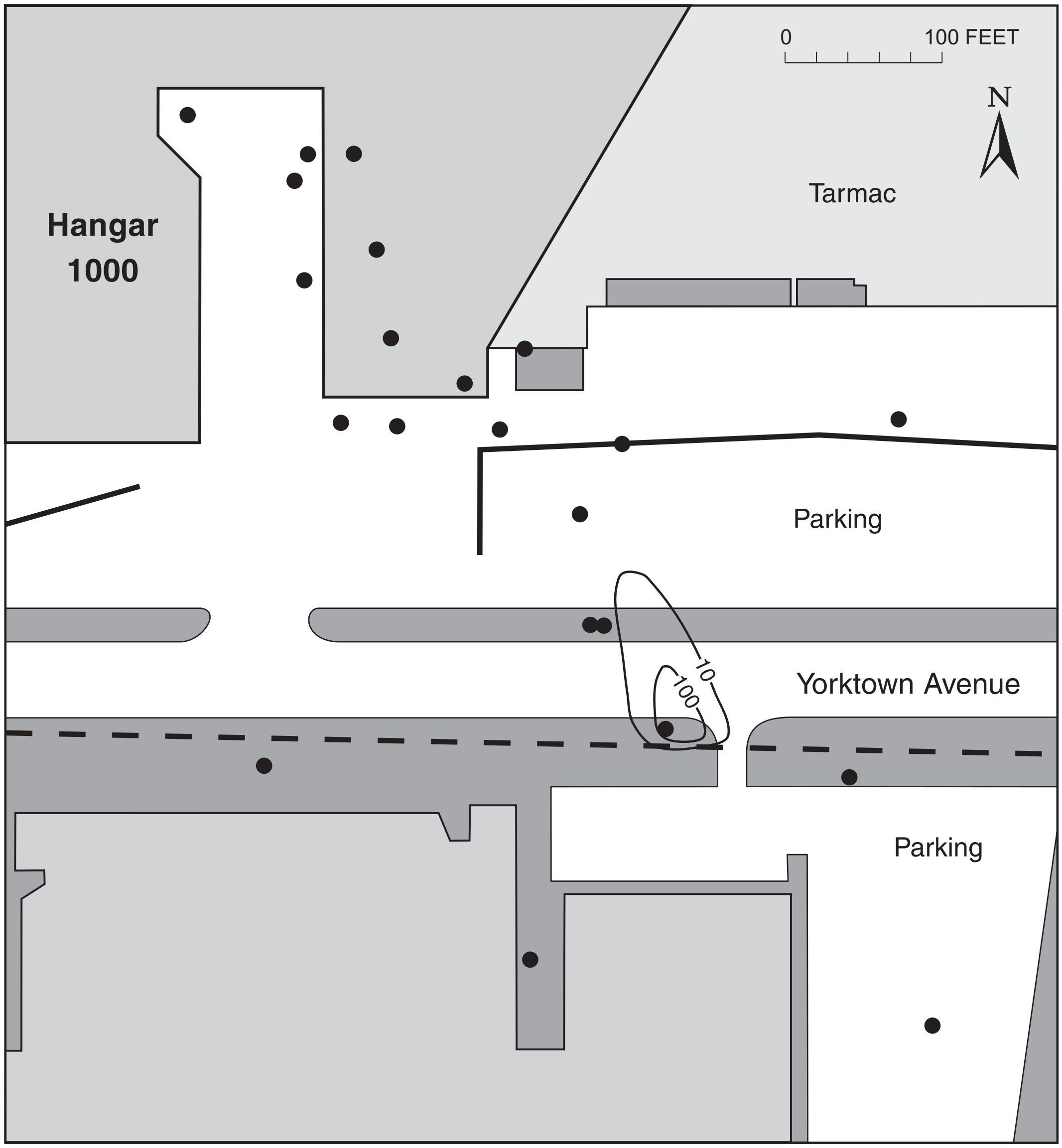

EXPLANATION

STORMWATER DRAINS THAT ARE NOT DRAINING GROUND WATER–From the upper layer of the surficial aquifer

STORMWATER DRAINS THAT ARE DRAINING GROUND WATER–From the upper layer of the surficial aquifer

10 LINE OF EQUAL SIMULATED TCE CONCENTRATION–In micrograms per liter. Interval is variable

MONITORING WELL LOCATION

Figure 44. Simulated trichloroethene (TCE) concentrations in layer 1 after 16 years assuming 100 percent source reduction.

If the actual ground-water velocities are greater than the simulated velocities, then the contaminants will move to the storm sewer faster than predicted; if the simulated velocities are slower, then the contaminants will remain in the aquifer longer and arrive at the sewer later than predicted. Ground-water velocity probably is the most important factor when predicting the traveltime from the source area to the storm sewer.

Simulated contaminant concentrations discharging to the sewer are related directly to initial concentrations at the source. The simulation will underpredict concentrations discharging to the sewer if measured concentrations in the source area are substantially higher than concentrations sampled from the wells. However, the plumes, which were generally well-defined laterally and vertically, were characterized using data from several wells, thus making it unlikely that higher concentrations existed.

Model parameters such as retardation, hydrodynamic dispersion, porosity, and chemical degradation have a strong influence on the simulated movement and concentration of contaminants. Variations in each of the these parameters can affect the model-simulated fate and transport of contaminants. As discussed previously, the organic carbon content was measured at three locations in the upper layer of the surficial aquifer. The organic carbon content was averaged to determine retardation factors used in model simulations. With only three samples, the actual range of values in the aquifer may not be well characterized and could vary from the values used. The effect of retardation on contaminant movement is straightforward. If the retardation factor is doubled, then the rate of travel of the contaminant is halved. Conversely, if the retardation factor is halved, then the rate of travel is doubled. For example, simulated concentrations of TCE at a traveltime of 8 years are shown in figure 37. If the retardation factor for this simulation were doubled, then the TCE would have traveled only one quarter of the distance to the storm sewer. Conversely, if the retardation factor were halved, then the plume would have reached the storm sewer.

Similar to the retardation factor, the effective porosity affects the movement of contaminants, but in a linear fashion. If the porosity is doubled, then the traveltime of the contaminants also is doubled. If the porosity is halved, then the traveltime is halved. For example, in figure 37, if the porosity for this simulation had been halved, then the contaminant plume would have reached the sewer. Conversely, if the porosity had been doubled, then the contaminant plume would have traveled only one quarter of the way to the sewer. Effective porosity is difficult to quantify in the field. The value used in this model was 25 percent, and could reasonably be expected to vary from about 12.5 percent up to about 30 percent.

The simulated first order rates of chemical degradation were 0.0002, 0.0002, and 0.06 d^{-1} for TCE, DCE, and VC, respectively. Because a similar rate of degradation for TCE was documented at a similar site nearby (U.S. Navy, 1998), using this rate has some justification. The rates for DCE and VC, however, are simply model-calibration parameters (although they fall within expected values) that resulted in the best calibration for the model. If the actual rates of degradation are substanially different (or if they vary over time), then the simulated concentration values also could vary substantially. In addition, the initial concentrations and simulated concentrations in the aquifer are correlated, thus making a unique prediction more difficult. For example, if the initial concentration were too high and the first order decay rate too low, then a match to the measured values might still be possible.

SUMMARY

The Jacksonville Naval Air Station occupies 3,800 acres adjacent to the St. Johns River in Jacksonville, Florida. Hangar 1000, in the north-central part of the Station is an area where aircraft are serviced and repaired. Two underground storage tanks containing solvents were operated from the late 1960s until they were closed in 1994. One tank was a 750-gallon concrete tank used as a solvent and water separator. The other was a 2,000-gallon steel tank that received solvent overflow from the first tank, and waste oils and solvents discharged from other operations at the facility. Both tanks, associated piping systems, and visually identified contaminated soils were excavated and removed in March 1994. However, tests indicated that solvents had previously leaked from the tanks into the ground-water system.

Ground-water samples at one of the tank sites had levels of trichloroethene (TCE) and dichloroethene (DCE) of 8,710 and 4,280 μg/L, respectively. Some of the DCE at the site is from the biodegradation of TCE, and all of the vinyl chloride (VC) at the site is derived from the biodegradation of DCE. Ground water at Hangar 1000 flows toward a storm sewer that drains ground water from the aquifer. Analyses indicate that TCE, DCE, and VC plumes are traveling with the ground water and have reached the storm sewer. The sewer discharges to a small creek, which discharges to the St. Johns River.

A subregional model was calibrated to simulate the ground-water flow in the region around Hangar 1000 using the Modular Three-Dimensional Finite-Difference Ground-Water Flow Model (MODFLOW). This model was then used to establish the boundary conditions for a site-specific ground-water flow model and a fate and transport model using the computer code, Reactive Transport in Three Dimensions (RT3D).

Model results indicate that the ground-water flow velocity averaged about 75 ft/yr and it took about 6 years for the ground water to travel from the tank removal site to the storm sewer. Modeling results also indicate that the traveltime from the tank removal site to the storm sewer is 16, 14, and 12 years for TCE, DCE, and VC respectively. TCE has the longest traveltime because it has the highest retardation factor of 2.5; DCE takes less time with a retardation factor of 2.0; and VC has the the fastest traveltime because it has the lowest retardation factor of 1.7. Modeling results indicate that the release of contamination in the aquifer occurred more than 16 years ago, and currently all three contaminants are at steady-state conditions; thus, plume locations and concentrations are not changing substantially at this time.

Model-derived dispersivity values for Hangar 1000 were: longitudinal 1.5 ft, transverse 0.27 ft, and vertical 0.27 ft. Because the discharge point was close to the source (about 450 ft), the model was relatively insensitive to dispersivity. This is because dispersivity has the greatest effect on contaminant concentrations over long distances. The model-derived first order decay rate for TCE at Hangar 1000 was 0.0002 d^{-1}. In a previous study at a similar nearby site, first order decay rates of 0.0007 to 0.0002 d^{-1} were determined. The calibrated first order decay rate was 0.0002 d^{-1} for DCE and 0.06 d^{-1} for VC. The expected range of values for VC is 0.002 to 0.08 d^{-1}.

The Navy has begun pilot tests to reduce the TCE and DCE concentrations at the tank removal site. Source reductions of 50 percent and 100 percent were simulated. As expected, reducing the contaminant source by 50 percent resulted in TCE, DCE, and VC concentrations that were half of their original concentrations. It took about 16 years for new steady-state TCE concentrations to develop, about 14 years for DCE, and about 12 years for VC. Reducing the source area concentrations by 100 percent in the model eventually resulted in the total elimination of TCE, DCE, and VC in the aquifer. The simulated period of time for the contamination to be removed from the aquifer once the source was removed was about 17 years for TCE, 15 years for DCE, and 13 years for VC.

REFERENCES

Brooks, H.K., 1981, Physiographic divisions, State of Florida: University of Florida, Center for Environmental and Natural Resources Programs, 1 sheet.

Clement, T.P., 1997, A modular computer code for simulating reactive multi species transport in 3 dimensional groundwater aquifer, Battelle Pacific Northwest National Laboratory REsearch Report PNNL-SA-28967

Davis, J.H., 2001, Documentation of three aquifer tests conducted at Hangar 1000, U.S. Naval Air Station, Jacksonville, Florida, U.S. Geological Survey Open-File Report, 20 p.

Davis, J.H., Planert, M., and Andrews, W.J., 1996, Simulation of ground-water flow at the U.S. Naval Air Station, Jacksonville, Florida, with an evaluation of changes to ground-water flow caused by proposed remedial designs at Operable Unit 1: U.S. Geological Survey Open-File Report 96-597, 47 p.

Davis, J.H., 1996a, Documentation of aquifer test conducted at Area D, Operable Unit 3, U.S. Naval Air Station, Jacksonville, Florida, U.S. Geological Survey Open-File Report, 30 p.

-----, 1996b, Documentation of aquifer test conducted at Area A, Operable Unit 3, U.S. Naval Air Station, Jacksonville, Florida, U.S. Geological Survey Open-File Report, 15 p.

-----, 1998, Ground-water hydrology and simulation of ground-water flow at Operable Unit 3 and surrounding region,U.S. Naval Air Station, Jacksonville, Florida: U.S. Geological Survey Open-File Report 98-68, 36 p.

-----, 2000, Fate and transport modeling of selected chlorinated organic compounds at Operable Unit 3, U.S. Naval Air Station, Jacksonville, Florida: U.S. Geological Survey Open-File Report 00-255, 36 p.

-----, 2001, Documentation of three aquifer tests conducted at Hangar 1000, U.S. Naval Air Station, Jacksonville, Florida, U.S. Geological Survey Open-File Report, 20 p.

Fairchild, R.W., 1972, The shallow-aquifer system in Duval County, Florida: Tallahassee, Florida Bureau of Geology Report of Investigations no. 59, 50 p.

Gelhar, L.W., Welty, C., and Rehfeldt, K.R., 1992, A critical review of data on field-scale dispersion in aquifers: Water Resources Research, v. 28, no 7, 19 p.

Hillel, D., 1980, Fundamentals of soil physics, Academic Press, Inc., 413 p.

Hseih, P. A., and Freckleton, J. R., 1993, Documentation of a computer program to simulate horizontal-flow barriers using the U.S. Geological Survey's modular three-dimensional finite-difference ground-water flow model: U.S. Geological Survey Open-File Report 92-477, 32 p.

McDonald, M.G., and Harbaugh, A.W., 1988, A modular three-dimensional finite-difference ground-water flow model: U.S. Geological Survey Techniques of Water-Resources Investigations, book 6, chap. A1, variously paged.

Mercer, J.W., Skipp, D.C., and Griffin, D., 1990, Basic pump-and-treat ground-water remediation technology: U.S. Environmental Protection Agency, EPA/600/8-90/003.

Miller, J.A., 1986, Hydrogeologic framework of the Floridan aquifer system in Florida, and in parts of Georgia, Alabama, and South Carolina: U.S. Geological Survey Professional Paper 1403-B, 91 p.

Pollock, D.W., 1989, Documentation of computer programs to compute and display pathlines using results from the U.S. Geological Survey modular three-dimensional finite-difference ground-water flow model: U.S. Geological Survey Open-File Report 89-381, 188 p.

Scott, T.M., 1988, The lithostratigraphy of the Hawthorn Group (Miocene) of Florida: Tallahassee, Florida Geological Survey Bulletin no. 59, 148 p.

U.S. Environmental Protection Agency, 1998, Technical protocol for evaluating natural attenuation of chlorinated solvents in ground water: Environmental Protection Agency EPA/600/R-98/128, 231 p.

U.S. Navy Department, Southern Division, Naval Facilities Engineering Command, 1994a, Remedial investigation and feasibility study, Operable Unit 3, Naval Air Station, Jacksonville: South Division Contract N62467-89-D-0317, 142 p.

-----, 1994b, Engineering evaluation and cost analysis buildings 106 and 780 at Operable Unit 3, Naval Air Station, Jacksonville: South Division Contract N62467-89-D-0317/076, 48 p.

-----, 1998, Engineering evaluation of areas with elevated groundwater contamination, Operable Unit 3, Naval Air Station, Jacksonville: South Division Contract N62467-89-D-0317/076, 107 p.

-----, in press, Remedial Investigation for Hanger 1000, Naval Air Station, Jacksonville: South Division Contract N62467-94-D-0888, 70 p.

Zheng, C, and Bennett, G. D., 1995, Applied contaminant transport modeling, theory and practice: New York, Van Nostrand Reinhold, 440 p.

Zheng, C, and Wang, Patrick, 1998, MT3DMS Documentation and user's guide: Tuscaloosa, Ala., Departments of Geology and Mathematics, University of Alabama, 185 p.